RESEARCH FOR DYNAMIC SEAL FRICTION MODELING IN LINEAR MOTION HYDRAULIC PISTON APPLICATIONS

by

BRIAN E. SUISSE

Presented to the Faculty of the Graduate School of

The University of Texas at Arlington in Partial Fulfillment

of the Requirements

for the Degree of

MASTER OF SCIENCE IN MECHANICAL ENGINEERING

THE UNIVERSITY OF TEXAS AT ARLINGTON

August 2005

ACKNOWLEDGEMENTS

The author would like to express his sincere thanks to Dr. Robert Woods for providing guidance and resources during the research phase of this thesis. In addition, the efforts of committee members B. P. Wang and Seiichi Nomura are also appreciated.

Appreciation is also extended to Rick Thoman for the reference material and general experience that was shared, John Frakes for assistance in test setup and execution, Elme Schmale and Trelleborg Sealing Solutions for assistance in providing finite element analysis data, and both Rohn Olson & Ken Bowthorpe for general support in procuring test hardware.

April 30, 2005

ABSTRACT

RESEARCH FOR DYNAMIC SEAL FRICTION

MODELING IN LINEAR MOTION

HYDRAULIC PISTON

APPLICATIONS

Publication No. _____

Brian Suisse, M.S.

The University of Texas at Arlington, 2005

Supervising Professor: Robert L. Woods

This paper presents a unique physics-based analytic model for dynamic seal friction in hydraulic actuators as a function of cylinder pressure, seal material, piston rod dimensions, piston rod seal gland dimensions, and other influencing factors.

Results from a series of friction tests are presented. Finite element analysis of an installed seal is used to predict contact stress between the seal and the gland, providing a normal force against the sealing surface. This information is used to determine coefficients of friction within the test specimen. From the analysis, a pressure-sensitive model is generated. The friction model is overlaid on the test data

and proves to be suitable for use in a hydraulic actuator simulation. Results from a simple closed-loop servo actuator model are then presented with friction effects included. Recommendations are proposed for further study and development to provide better versatility in dynamic seal friction modeling.

TABLE OF CONTENTS

LIST OF ILLUSTRATIONS

LIST OF TABLES

CHAPTER 1

INTRODUCTION: SEAL FRICTION

1.1 Seal Friction Effects

Traditionally, seal friction in a dynamic hydraulic system has been predicted using very simplified assumptions. In the case of a hydraulic actuator piston rod seal, the friction force is usually approximated as a constant value. This value may be determined through testing by cycling an unpressurized actuator with an external load and measuring the force required to move the piston. In some cases, the total friction value is determined by slowly raising the pressure applied to a cylinder port until the piston moves. The pressure is then divided by the effective piston area to produce a friction force. The friction force value is typically incorporated into the model as a constant force opposing the direction of piston motion, or given the value of zero if the piston is not moving.

1.2 Deficiencies in Predicting Seal Friction

Such a simplified approximation of friction as described in section 1.1 may not be sufficient to produce accurate results in certain system models where friction forces are large compared to actuator output forces. Friction due to dynamic seals used in hydraulic systems is largely dependent on applied pressure and seal installation forces. Other factors, such as hydraulic fluid types, hardware temperature, sealing surface

finishes, seal material, and duration of seal contact should be considered as well. In addition to physical considerations, friction states must be incorporated into a model for better fidelity of results.

1.3 Contributors to Seal Friction

Physical parameters, such as seal groove dimensions, piston dimensions, seal dimensions, and seal hardness will determine the contact stress imposed by installation of the seal. Interference fit between a seal and the groove boundaries is specified in percent squeeze. The percent squeeze is the amount of compression on an installed seal as compared to its original cross-sectional diameter. For the purposes of simplicity, this evaluation will consider a standard O-ring installed into a standard piston rod sealing groove. Figure 1 shows a typical O-ring that may be used for sealing a piston rod. On a balanced piston actuator, an O-ring is installed into a seal groove on each end of the hydraulic cylinder and the piston rod is installed through the I.D. (inner diameter) of the O-ring.

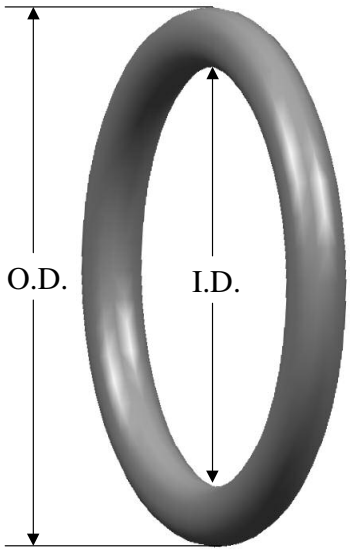

Figure 1 O-Ring

The important dimensions for specifying an O-ring, a piston diameter, and a seal groove are shown in Figure 2.

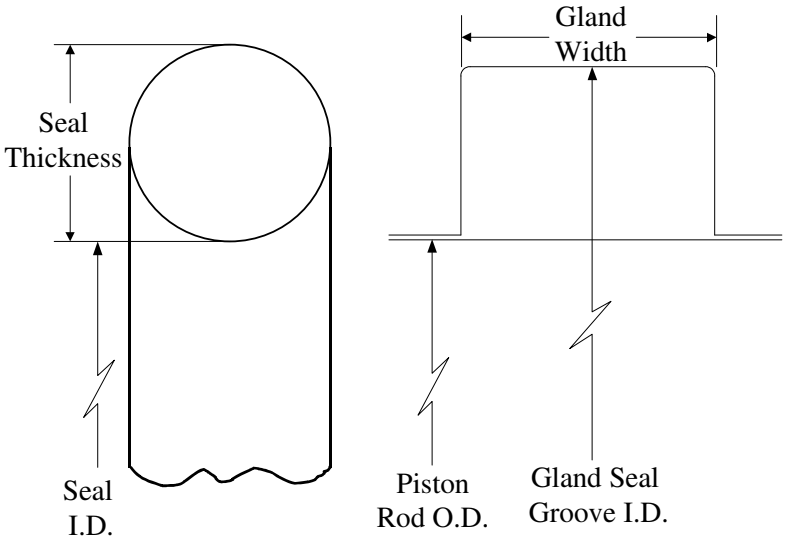

Figure 2 O-Ring and Installation Groove

In a balanced area actuator assembly, the dynamic piston rod seals are located on each end of the cylinder within the end glands. The piston is allowed to slide axially, relative to the cylinder. Figure 3 shows a typical arrangement for a balanced area actuator.

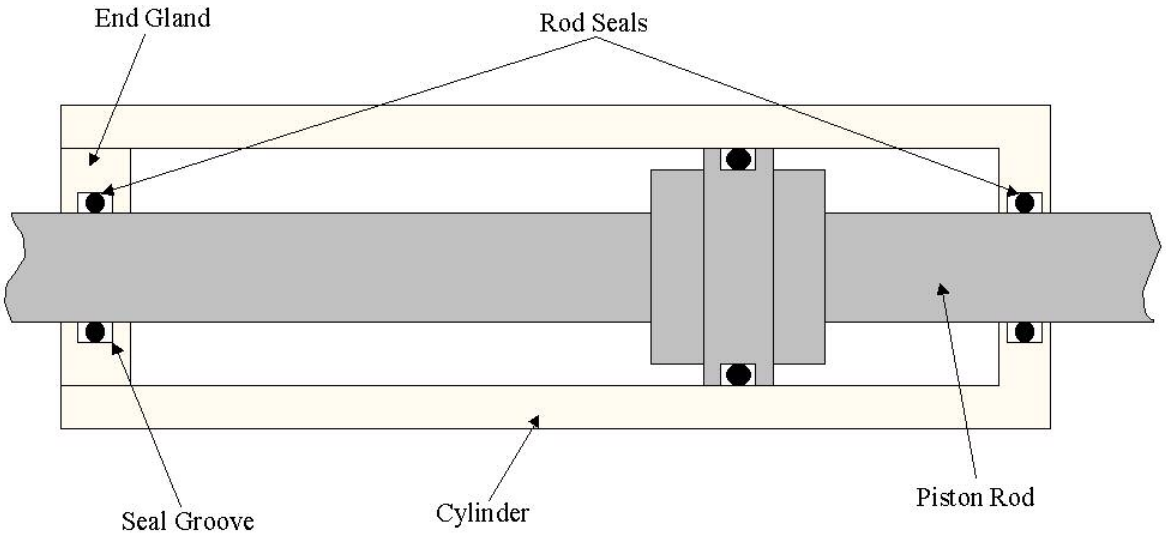

Figure 3 Actuator Internal View and Seal Locations

Upon installation into the gland seal groove, the O-ring becomes compressed, producing contact stresses between the seal I.D. and the piston rod O.D. (outer diameter). The contact stress produces a normal force when integrated over the length of contact (L_c), which, when multiplied by a coefficient of friction, causes a Coulomb friction force that opposes the net force applied to the piston. See Figures 4-6.

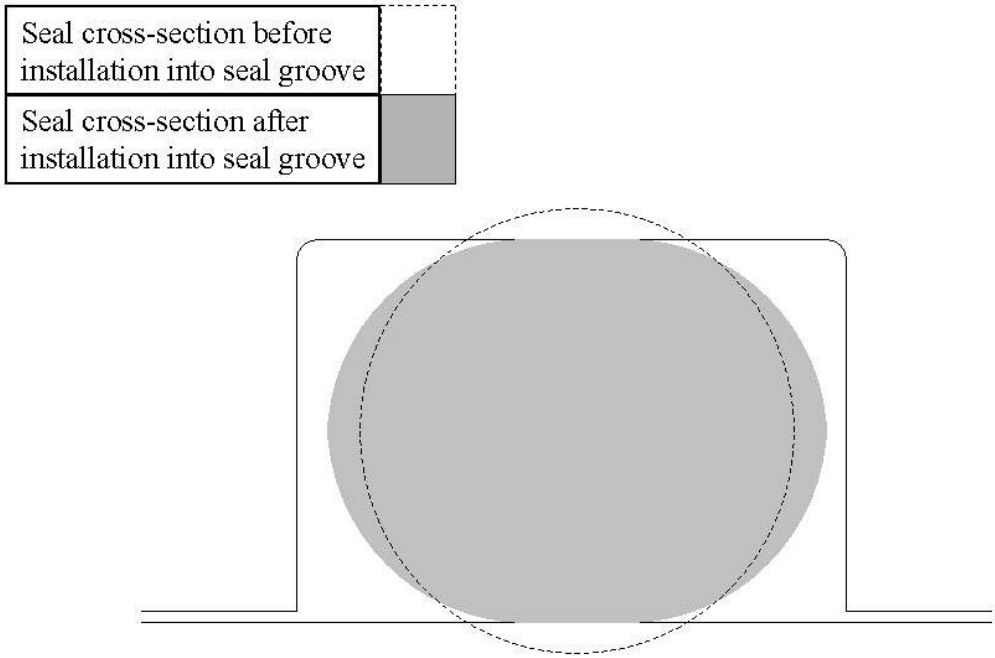

Figure 4 O-Ring Installed in Groove

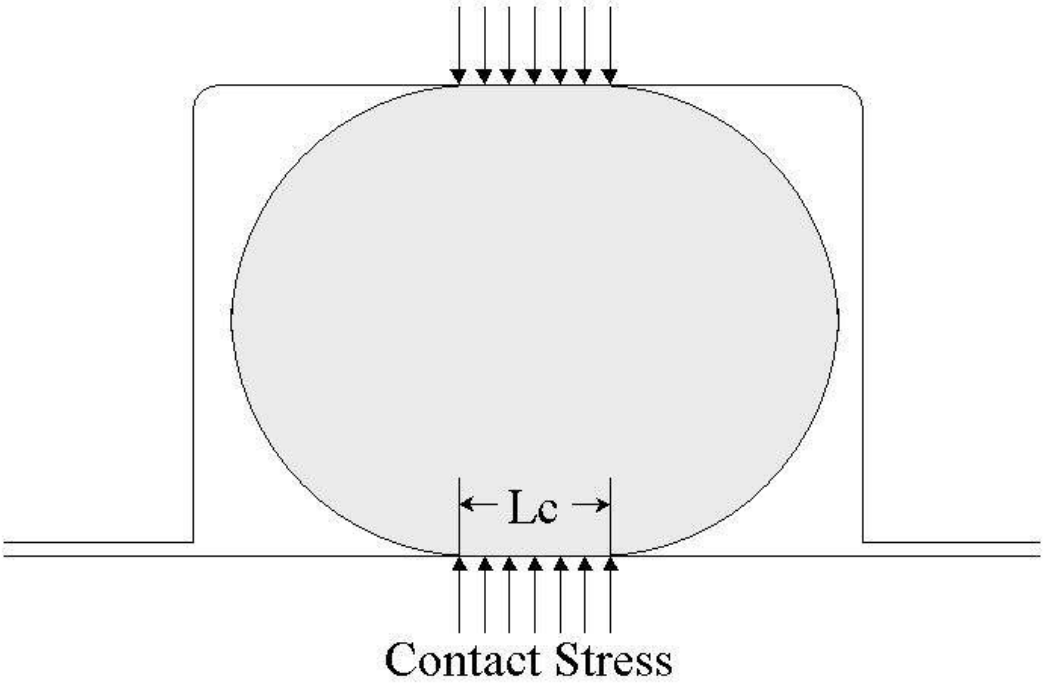

Figure 5 Contact Stress

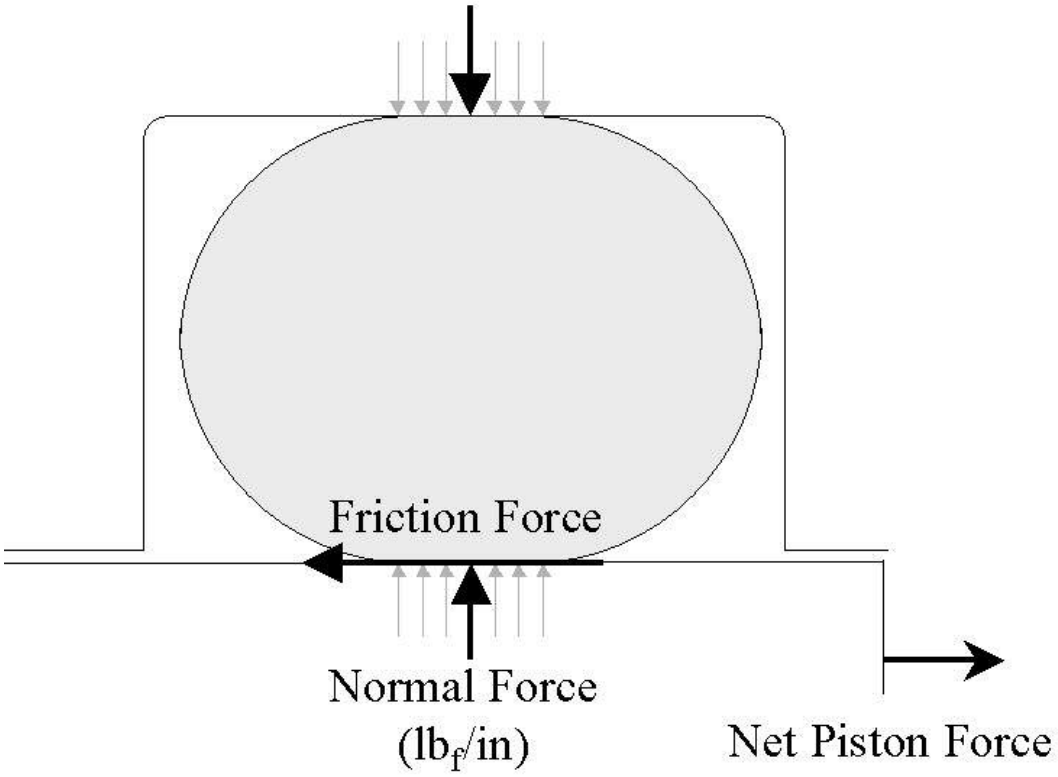

Figure 6 Normal Force and Coulomb Friction Force

As pressure is applied to the cylinder, the O-ring seats against the face of the groove. As pressure increases, the O-ring deforms and conforms to the shape of the groove. The contact stresses resulting from the reaction to pressure and this deformation cause increased normal force on the sealing face, as well as an axial force from the seal groove face. Figures 7 and 8 illustrate forces and stresses on the seal as a result of cylinder pressure.

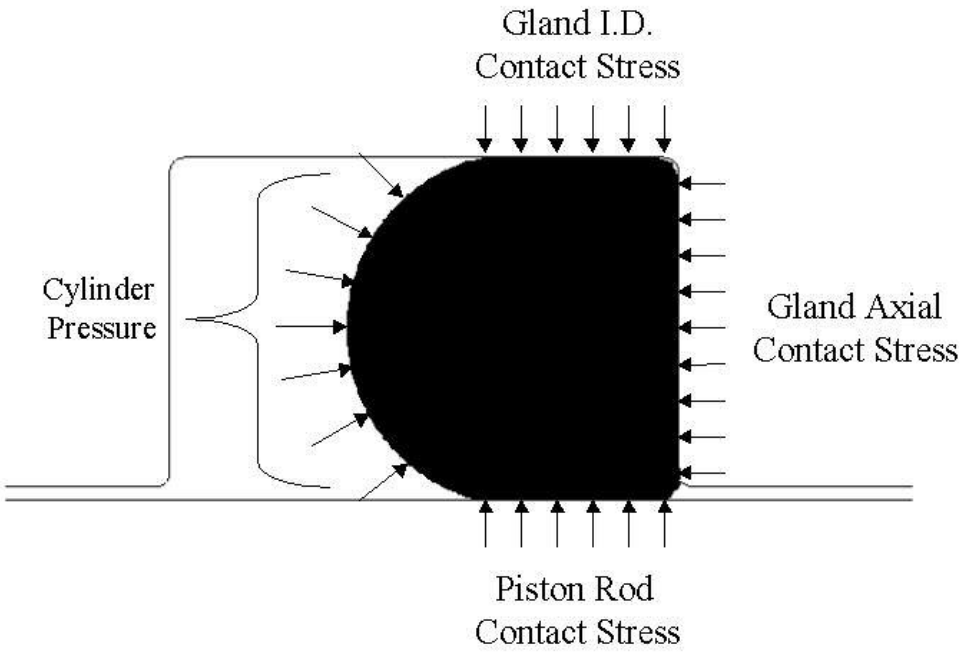

Figure 7 Contact Stresses Due to Cylinder Pressure

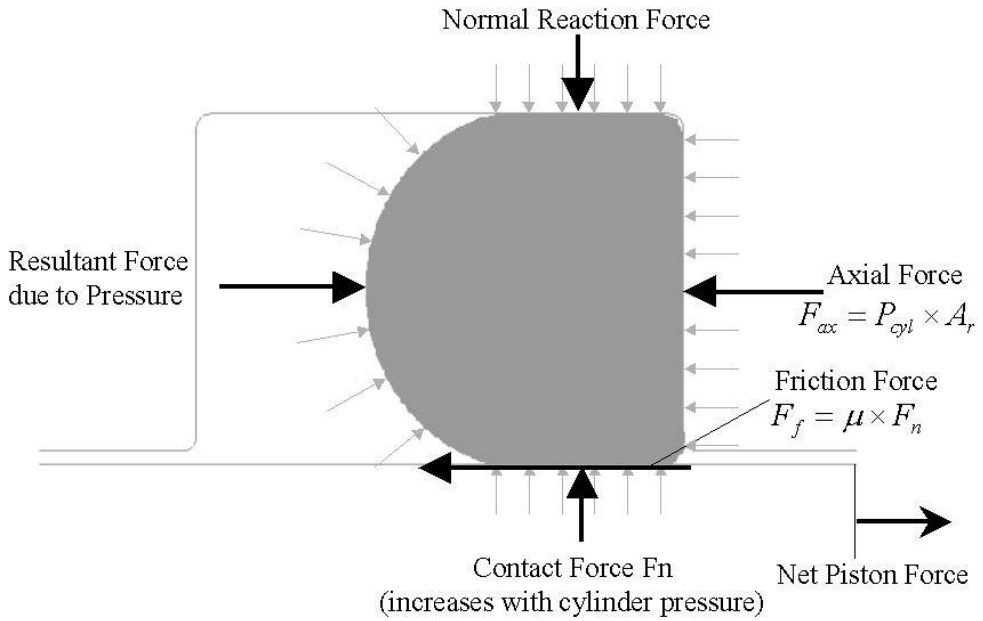

Figure 8 Normal Force and Coulomb Friction Force

CHAPTER 2

PRIOR ART METHOD OF PREDICTING SEAL FRICTION

2.1 Calculation Method from Literature

A commonly accepted method (2,3) of predicting coulomb friction between a seal and a piston rod incorporates the use of curves that isolate the friction due to seal squeeze and the friction due to pressure. The friction value is given by the following sum:

$$F = F_C + F_H$$

Descriptions of important parameters in this method are given in Table 1.

Table 1 Friction Calculation Parameters

Parameter	Value	Description
F_C	f_c x L_r	Total friction force due to seal squeeze
F_H	f_h x A_r	Total friction force due to pressure
f_c	Given in Figure 9	Friction (lb_f per inch seal contact length)
f_h	Given in Figure 10	Friction (lb_f per $inch^2$ seal projected area)
L_r	π x Piston O.D.	Piston circumference
A_r	$\pi/4$ x ((Gland I.D.)^2-(Rod O.D.)^2)	Seal projected area (see Figure 11)

The friction per inch length (f_c) of the seal due to seal squeeze is given in Figure 9. Figure 10 gives the friction per square inch of the seal projected area (f_h) due to cylinder pressure.

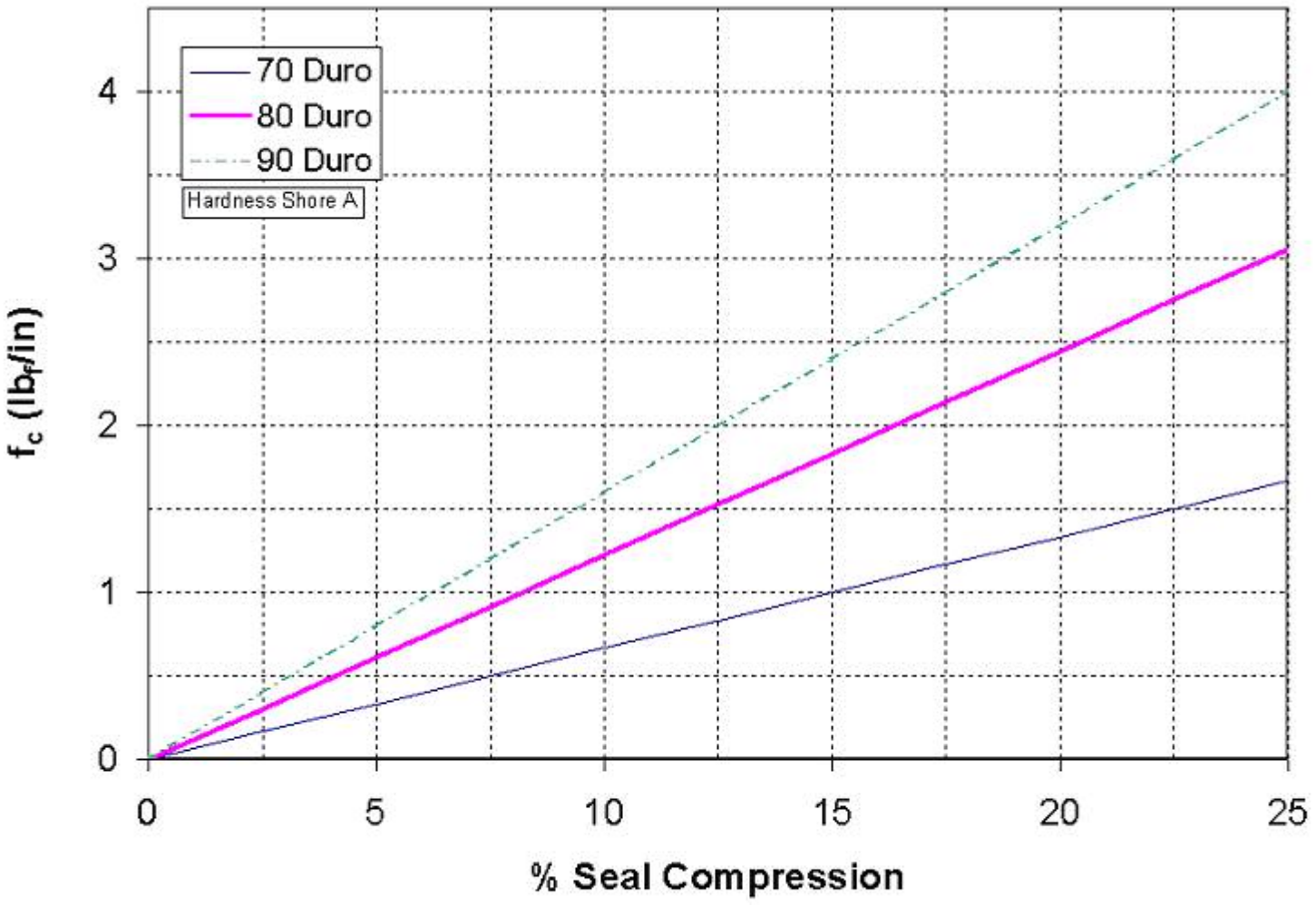

Figure 9 Friction Due to O-ring Compression

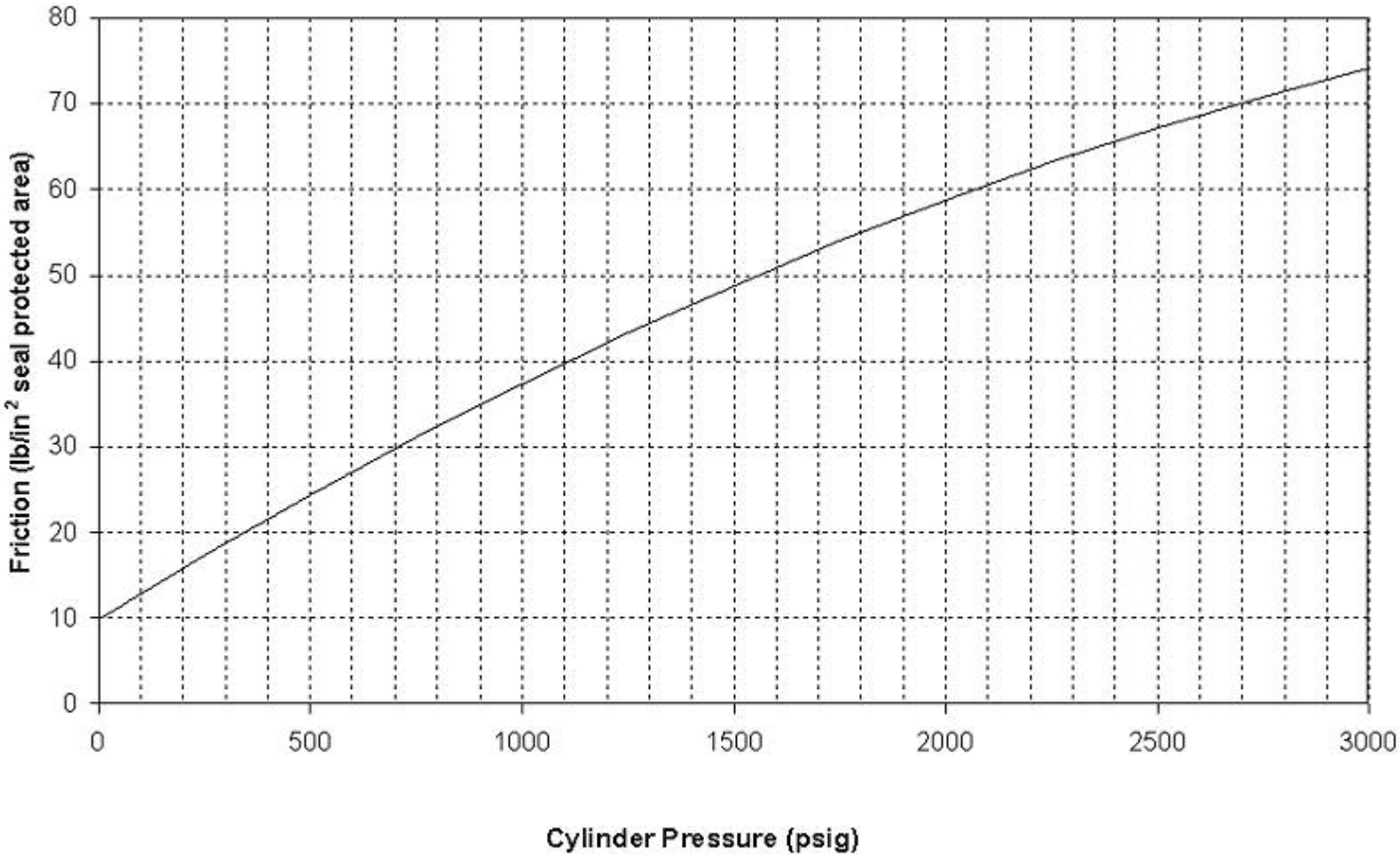

Figure 10 Friction Due to Cylinder Pressure

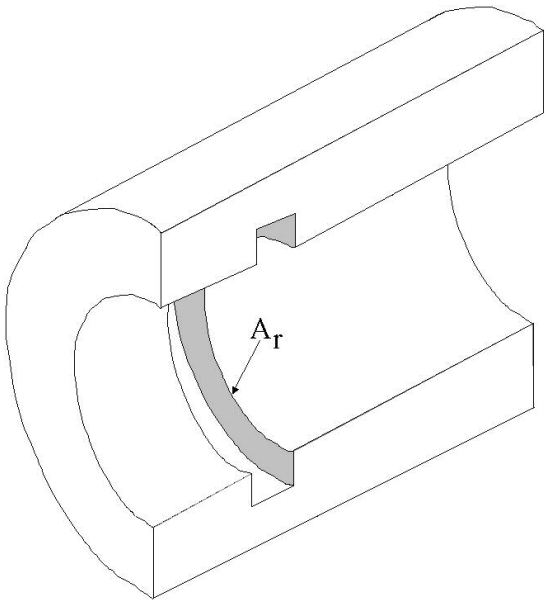

Figure 11 Projected Area A_r within a Seal Groove

2.2 Friction Calculation Results from Prior Art Method

The method described in section 2.1 of this evaluation was used to characterize the friction forces in a system with known geometric and physical properties. A comparison with actual test data from Appendix A is given in Chapter 5.

The calculations were set up for an input pressure range of 0 to 1000 psi cylinder pressure. Using the dimensions from an existing actuator, as well as the physical properties and dimensions from the seals installed in the actuator, the input parameters were defined. Figures 10 and 11 were used to determine the values of F_c and F_h for the calculation of F. The input parameters are given in Table 2. The calculation output values are shown in Table 3 and a chart depicting the friction force as a function of pressure is given in Figure 12.

Table 2 O-Ring Seal Friction Calculation Constants

Measured Parameters		Calculated Parameters		Chart Values	
Parameter	Value	Parameter	Value	Parameter	Value
Seal Thickness (in)	.106	Ar (in^2)	.223	f_c (lb_f/in)	0.5
Gland O.D. (in)	.821	Seal Squeeze (%)	8		
Piston Rod I.D. (in)	.625	L_r (in)	1.96		
Seal Shore A Hardness	70	F_c (lb_f)	.99		

Table 3 O-Ring Seal Friction Calculation Variables and Output Values

Pressure (psi)	f_h (lbf/in^2)	F_H (lb_f)	F (lb_f)
0	9.9	2.2	3.2
100	13.0	2.9	3.9
200	15.9	3.5	4.5
300	18.8	4.2	5.2
400	21.6	4.8	5.8
500	24.4	5.4	6.4
600	27.1	6.0	7.0
700	29.9	6.6	7.6
800	32.3	7.2	8.2
900	34.9	7.8	8.8
1000	37.3	8.3	9.3

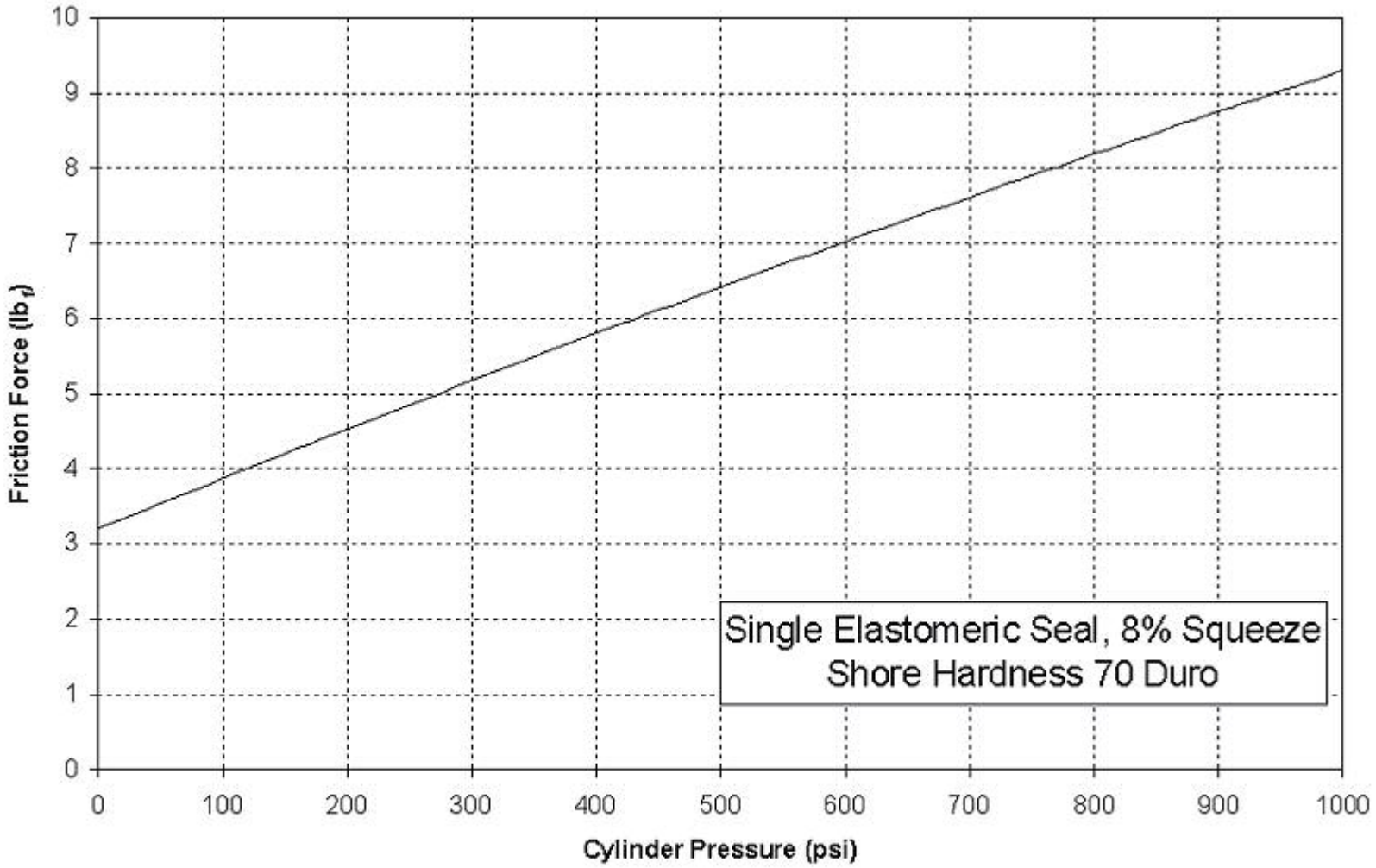

Figure 12 Dynamic Friction Force vs. Cylinder Pressure

2.3 Method Limitations

Although the method used in this chapter produces reasonable results, it has limitations. One drawback that may be apparent to the user is the need for charts. In order to calculate the values of F_C and F_H, the f_c and f_h data from the charts must be read and entered into a look-up table or a curve fit.

The other disadvantage is the fact that very minimal industry data is available for determining f_c and f_h. In addition, since the displayed data is already in the form of friction forces, coefficients of friction cannot be determined. It becomes more difficult to understand the phenomena internal to the sealing system that affects seal friction and sealing forces.

CHAPTER 3

FUNDAMENTAL CONTRIBUTIONS OF THIS THESIS

A unique seal friction model for use in dynamic hydraulic system analysis is defined herein. This model has been built using logical methods to improve the calculation of friction within a system.

In order to increase the fidelity of a model, a number of considerations should be made. The first is to make the friction calculation dependent upon pressure. Characterization of the contact stresses and resultant forces, along with coefficients of friction for a seal undergoing pressure changes is accomplished through analysis and testing.

It is important to consider the mechanisms by which seal friction is affected. Seal friction models can be refined by using a physics-based approach for predicting the normal force imposed on a seal during use. For example, an input parameter that should be included in a refined friction model is the percent squeeze on the installed seal.

Another factor that influences the effect friction has on a system is the method by which the friction states are defined. There are six unique logic states (1) that may be used to relay the value of the frictional forces within a system. These states are further discussed in Chapter 7.

The primary objective of this evaluation is to develop a dynamic model whereby frictional forces may be predicted in a hydraulic actuator piston rod seal. Through the

fulfillment of this objective, a useful tool will be gained to aid in simulating hydraulic power control systems.

The second objective is to better understand the mechanisms by which friction is generated in an O-ring under pressure. This will be accomplished through testing, analysis and predictions using finite element analysis.

The third objective is to determine the friction coefficients between a nitrile rubber O-ring and lapped chrome as the normal force varies. It has been observed that as force between a rubber compound and the mating surface increases, the friction coefficient decreases.

CHAPTER 4

BUILDING A PHYSICS-BASED MODEL

4.1 Important Parameters to Characterize

The ultimate goal of building a physics-based model is to find the axial friction force between the piston rod and the installed O-ring seal. In order to accomplish this, the total normal force on the seal must be determined. When installed and pressurized, the compressed seal exerts a radial squeeze on the piston rod. The gland / seal arrangement has a uniform cross-section around its circumference such that the value of the normal force can be determined by multiplying the radial force in pounds per inch by the length of the seal face in contact with the piston rod.

Various factors can influence the radial force (or normal force) on the O-ring. The first, as is the basis for this evaluation, is cylinder pressure. As the pressure increases, the seal seats against the face of the seal groove (see Figure 11, section 2.1). Although the rubber material may deform, the total volume of the seal can be assumed to be constant. This flows down to the two-dimensional case of the cross-sectional area of the O-ring as well. As pressure increases, the cross-sectional area of the O-ring stays constant. As the seal seats further into the gland face the internal stress increases within the seal and the external contact stresses between the O-ring and containment material (piston and seal groove) increase as well. Integrating the contact stress across the contact area between the O-ring and the piston rod surface provides a normal force.

Other dimensional limitations in the seal groove and piston rod contribute to the normal force on the O-ring. The installation squeeze on the seal is the cause of some of the stress on the seal. The squeeze is the percent compression, in length, of the O-ring cross section. This can be determined by the following formula:

$$\%Squeeze = \frac{OD_{seal} - \frac{\left(ID_{gland} - OD_{rod}\right)}{2}}{OD_{seal}} \times 100$$

Where OD_{seal} is the cross-sectional diameter of the O-ring, ID_{gland} is the end gland seal groove inner diameter, and OD_{rod} is the outer diameter of the piston rod. The contact stress between the piston rod and the seal can be integrated across the contact area to provide an installation normal force.

Another contributor to installation force on the seal is the radial stretch of the O-ring. Typically, the outer diameter of the piston rod is greater than the inner diameter of the O-ring. This is done to keep the seal from bunching or kinking when installed inside a seal groove. The interference fit between the piston rod and the O-ring creates a tangential force (or stretching force) on the O-ring. This occurrence is similar to hoop stress observed in a pressurized cylinder (4). The relationship is shown in Figure 13. Knowing the dimensions of the seal and piston rod, the elongation of the seal wrapped around the rod can be determined. From the elongation, a strain value can be calculated and multiplied by the modulus of elasticity of the nitrile rubber. This product represents the tensile stress (similar to the hoop stress on a pressurized cylinder) on the seal. Multiplying this stress by the cross-sectional area of the seal gives the tangential

(tensile) force on the installed seal. The explanation shown in Figure 13 gives the relationship between the total radial force exerted on the O-ring and the tangential force.

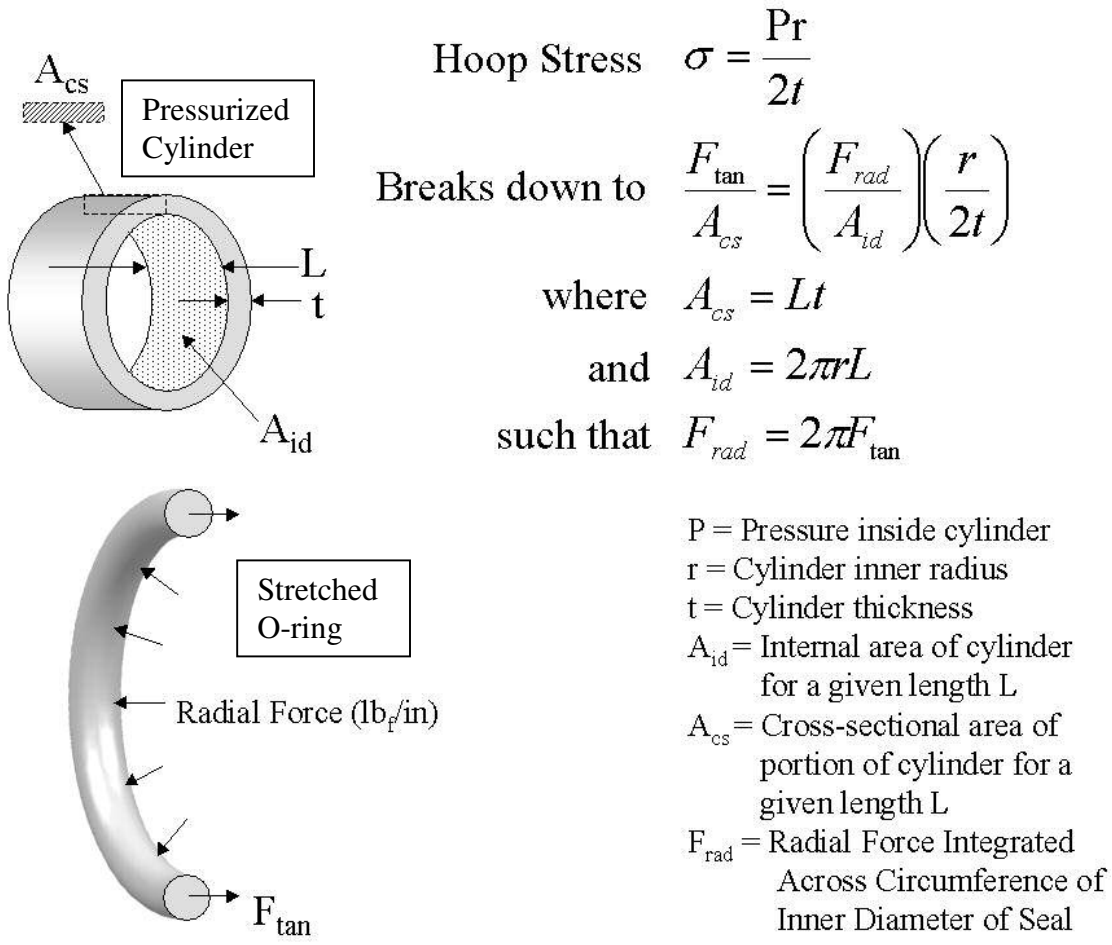

Figure 13 Similarities Between a Pressurized Cylinder and an O-Ring Stretched Radially

Another parameter that is required to build a friction model is the coefficient of friction. Between rubber and lap-finished chrome, the coefficient of dynamic friction, commonly denoted by μ, is observed to vary with normal force. For this reason, it

becomes logical to perform a series of tests to characterize the effects of normal force on frictional coefficients. These tests are further discussed in Chapter 5.

4.2 Using FEA Modeling for Determining Contact Forces

In an effort to record the relationship between cylinder pressure and contact forces (both normal and axial) on the O-ring, a series of finite element analysis (FEA) models were built and analyzed. Since the O-ring, seal groove, and piston surface cross-sections are uniform, an axisymmetric FEA model is adequate. Results from the Finite Element models are found in Appendix B.

The first model is the case of an installed O-ring with no cylinder pressure applied. Figure B-1 shows the contact stress on the O-ring. The deformation and contact stress in the FEA are due solely to the interference fit of the O-ring thickness inside the seal groove and against the piston rod surface. The pressure in the analysis is given in MPa and is converted to psi for the purposes of this evaluation. Using the FEA results, the contact stress is integrated over the contact length to give a force in lb_f per unit length. Since the stress is integrated over the two dimensional contact length across the cross section of the seal, the resultant force needs to be multiplied by the circumferential contact length of the O-ring on the piston rod. This yields the total normal force on the seal due to installation squeeze. Stresses and forces are given as part of a comparison in Chapter 6. Figure B-2 shows a side-by-side view of the analysis results for contact stress and Von Mises stress in the unpressurized installed seal case.

Five FEA models were built and analyzed for the purpose of determining contact stresses, and subsequently, resultant normal and axial forces on the O-ring under various pressurized cases. The first case has already been explained. The second through fifth cases are for the installed seal under cylinder pressures of 250, 500, 750, and 1000 psi, respectively. It is observed that as the cylinder pressure increases, the calculated normal force on the O-ring increases linearly as a function of pressure. Figures B-3 through B-6 illustrate the contact and Von Mises stresses in the seal for the second through fifth cases.

It should be noted that in all five cases, the surface sections of the seal that experience the most deformation are also subjected to the highest contact stresses. For each case, the contact stresses are integrated over the contact areas to produce the axial and normal forces on the seal. The tabulated results are given in Appendix B, Figures B-7 through B-11. Chapter 6 uses these normal force values, summarized below in Table 4 and Figure 14, in conjunction with seal friction test data to determine coefficients of friction.

Table 4 Summary of Normal Forces

Case	**Cylinder Pressure (psig)**	**Normal Force F_n (lb_f)**
1	0	4.1
2	250	22.4
3	500	44.5
4	750	67.2
5	1000	91.1

A linear relationship between seal normal force and cylinder pressure is given in Figure 14.

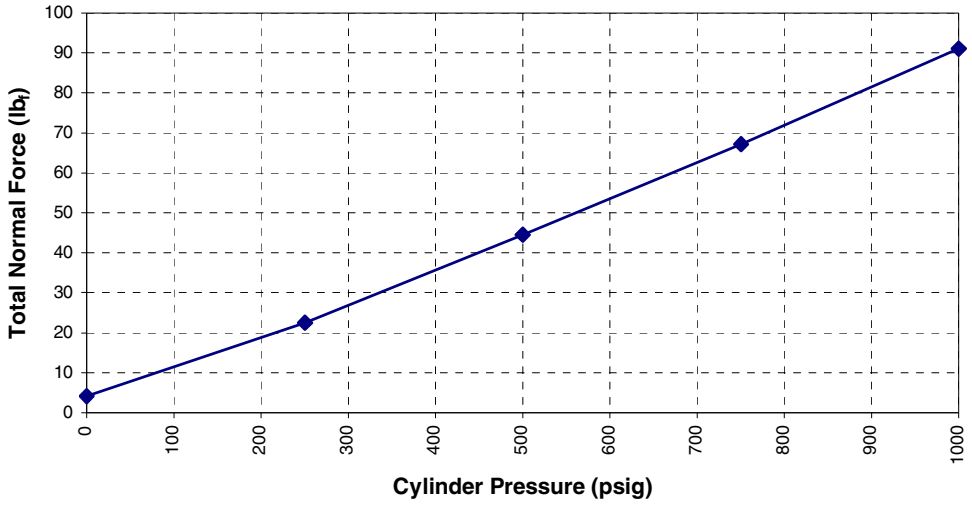

Figure 14 Total Normal Seal Force vs. Cylinder Pressure

CHAPTER 5

O-RING SEAL FRICTION TESTING

5.1 Test Setup

A representative actuator was used for friction testing. The previous calculations from Chapter 2 and the FEA introduced in Chapter 4 were performed using dimensions and materials matching those in the test actuator.

A test plan was written for the measurement of seal friction within the actuator specimen. The test plan is given in Appendix A. The test actuator is a balanced area actuator with cylinder feed ports drilled through the piston itself. A manifold block fits on the end of the piston with standard ports to feed both cylinder halves with pressure. The piston head seal was removed to ensure that the only friction force between the piston and the cylinder was the seal friction. An MS28775-114 O-ring was placed inside each cylinder end gland within the seal groove. Mil-H-5606 oil (red oil) was used as the hydraulic fluid. The piston end was fixed to a ground point and the cylinder was used as the moving member. Figure 15 illustrates the arrangement of the actuator specimen.

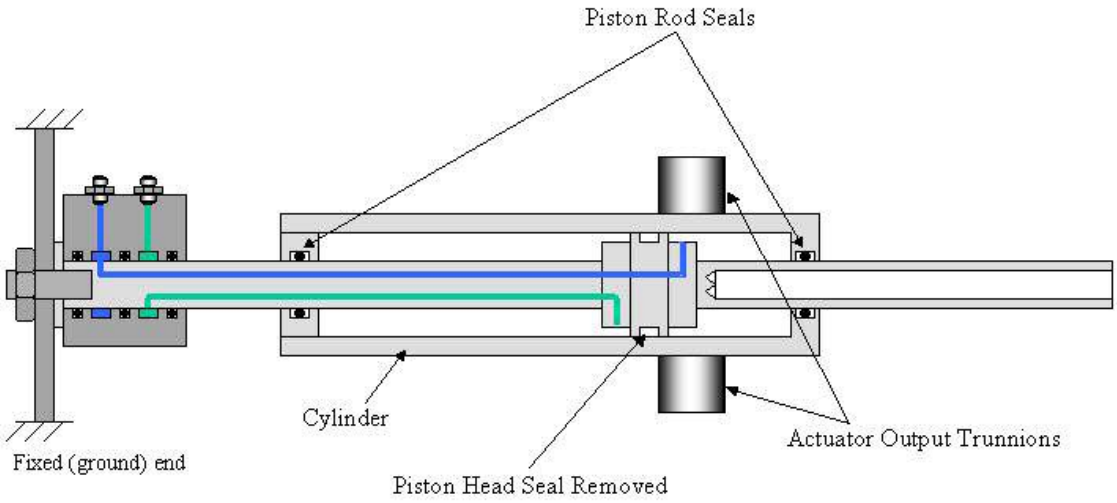

Figure 15 Test Specimen Actuator Arrangement

The manifold block was connected with hoses and fittings to interconnect the actuator cylinder ports, as well as supply both ports with pump pressure. A pull strap was fastened to the actuator output trunnions on the cylinder. A calibrated bi-directional 50 lb_f spring scale was used to move the cylinder. The friction force was measured using the spring scale. Figure A-1 in Appendix A shows the hydraulic connection and spring scale arrangement as used with the test specimen actuator. Figure A-2 is a photograph of the test specimen and Figure A-3 depicts an actual friction test. The hydraulic source pressure gage is shown in the bottom left corner of Figure A-3.

5.2 Test Procedure

The test specimen was cycled numerous times to allow the seals to seat properly within their grooves. This also caused the piston rod surface to become lubricated with a very thin film of hydraulic fluid. The cylinder was pressurized to 100 psig. This was done to assure that the seals would hold pressure and seat properly when pressurized. The pressure was then brought back to 0 psig. The first data points were taken at 0 psig cylinder pressure. The spring scale was used to extend the actuator by pulling on the trunnion strap. Static (breakout) friction was measured, along with dynamic (running) friction. The friction values were recorded. The actuator was allowed to sit for thirty seconds, then the spring scale was used to push on the cylinder end gland. Static and dynamic friction values were measured and recorded. The pressure was increased in 100 psi increments, with extend and retract direction static and dynamic friction values taken and recorded for each increment. Every data point was taken following a thirty second delay for consistency. It is observed that as rubber seals are allowed to sit in contact with their sealing surfaces, the friction required to move the actuator increases.

Friction data was taken for pressures up to 1000 psig, then pressure was reduced back to 0 psig. The test procedure was repeated two other times to show repeatability of the test data points. It was found that static friction, on average, was approximately 1 lb_f greater than dynamic friction (or 0.5 lb_f at each seal).

5.3 Test Data

Three different tests were performed for each discrete pressure value within the full pressure range. Results were recorded and tabulated. Friction test values are presented in Appendix A, Tables A-1, A-2, and A-3. The data is reported at 0.5 lb_f resolution.

It was observed that the breakout force (static friction) in the retract direction averaged 1.0 lb_f greater than the average static friction force in the extend direction. The dynamic case averaged 0.2 lb_f greater in the retract direction than in the extend direction. This difference is likely partially due to manufacturing tolerances in piston rod cross-sectional areas, as a differential rod area under pressure will create a small net force in one direction.

The static friction data is plotted in Figure A-4. The data for dynamic friction is plotted in figure A-5.

The static and dynamic friction test values were plotted on the same chart to illustrate the small difference between the value trends. A second order least-squares curve was used for a visual correlation between the basic trend of both types of friction. See Figure 16. For the purposes of this evaluation, the difference between static friction and dynamic friction will be referred to as “stiction”. Typically, stiction is the static friction in a hydraulic system, but the nomenclature is appropriate for the difference between static and dynamic friction when modeling the two.

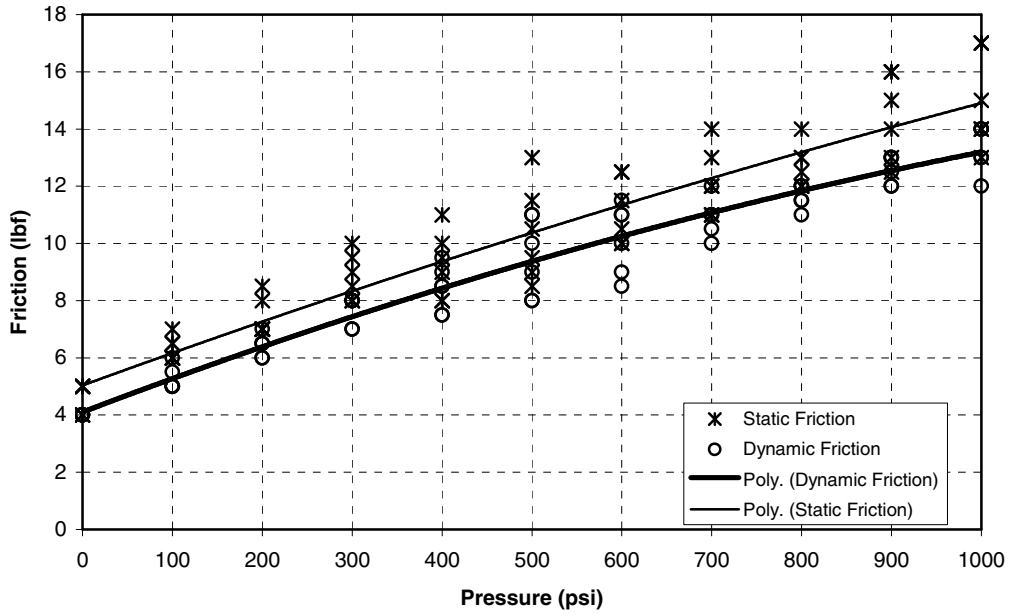

Figure 16 Static and Dynamic Friction vs. Pressure – All Three Tests

5.4 Comparison between Test Data and Prior Art Predictions

In order to evaluate the accuracy of the prior art friction calculation method discussed in Chapter 2, a comparison was made between calculated results and test results. The dynamic friction values in Table 3 were doubled to make a valid comparison with the test data, where the tests were performed using two O-ring seals under the same pressure. Figure 17 shows the prior art model overlaid on the test data.

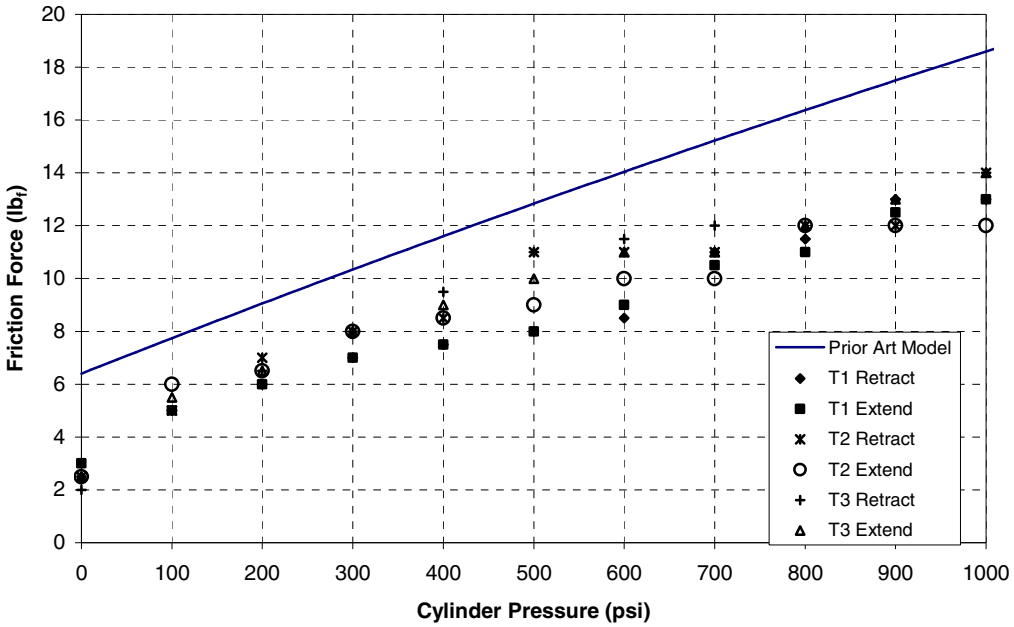

Figure 17 Prior Art Model and Dynamic Friction Data vs. Pressure

Note that the model overpredicts the dynamic friction by values ranging from 2 lb_f to 6 lb_f over the tested pressure range. The discrepancy can be related to lack of more comprehensive f_h and f_c data curves. While this method predicts conservative dynamic friction forces, the need still remains to further refine a seal friction model such that predicted values more closely match actual values.

CHAPTER 6

PREDICTING FRICTION COEFFICIENTS

6.1 Combine FEA and Test Results to Calculate Friction Coefficients

In order to draw a relationship between friction force and cylinder pressure, it becomes necessary to determine the coefficients of friction for the sealing system. A round, flexible cross-section is difficult to characterize when installed within a confining geometry, then pressurized. As such, the process of merging the friction test results from Chapter 5 with the FEA results from Chapter 4 is not an unreasonable method for characterizing the seal behavior under pressure.

The FEA models briefly described in Chapter 4 are analyzed in Appendix B to determine the axial and normal forces on the seal for a pressure range varying from 0 to 1000 psig. For each case, the length of seal that contacts the piston rod surface is recorded. The contact pressure is then integrated over the contact length to give a normal force in pounds force per inch. A total normal force is determined by multiplying this value by the circumferential contact length of the seal on the piston rod surface. The axial force is a simpler calculation and does not require any integration because it is equal to the cylinder pressure value multiplied by A_r (A_r is shown in Figure 11, Chapter 4). Figures B-7 through B-11 contain the data extracted from the FEA models. Each of these figures represents a case in which the seal is subjected to a cylinder pressure between 0 and 1000 psig. Note that each case gives a total axial force F_{ax} and a total normal force F_n exerted on the deformed seal.

The "Cell Contact Area" in Figures B-7 through B-11 represents the area of each cell that contacts the piston rod in the deformed state. This value is necessary because the FEA is performed as a two-dimensional axisymmetric model. The cell contact area is determined by multiplying the cell / piston rod contact length by the circumference of the piston rod. The contact stress values calculated during the finite element analysis are given in these figures for each cell. The "Cell Force" column refers to the normal force (the radial piston rod force) around the cell contact area for each cell. This value is the product of the contact stress and the cell contact area. When summed across the entire seal / piston rod contact length, a total normal force is yielded. This normal force is correlated with the friction test data referenced in Chapter 5 to determine coefficients of static and dynamic friction. The charts shown in Figures B-7 through B-11 are representations of the contact stress at each cell. The x-axes of the charts represent node positions relative to the point where the seal starts to contact the piston rod on the pressurized side of the seal. The term "node" is used to describe the center point of each cell. Each node provides a reference point along the contact length.

The combination of the normal force, along with the test friction values from Chapter 5 gives an understanding of how the coefficient of friction, μ, changes with normal force in a rubber seal. A more appropriate relationship would be between μ and contact stress for an area that has roughly uniform contact stress. In this case, the stress varies widely across the contact length of the seal due to the circular cross-section and large deformations of the material in local regions. For the purposes of this evaluation, the normal force will be used instead of contact stress. The normal force, after all, is the

integration of the contact stress over the contact area. Figure 18 illustrates the behavior of the coefficient of dynamic friction as normal force increases on the O-ring. Note that as force increases on the seal, the dynamic friction coefficient decreases.

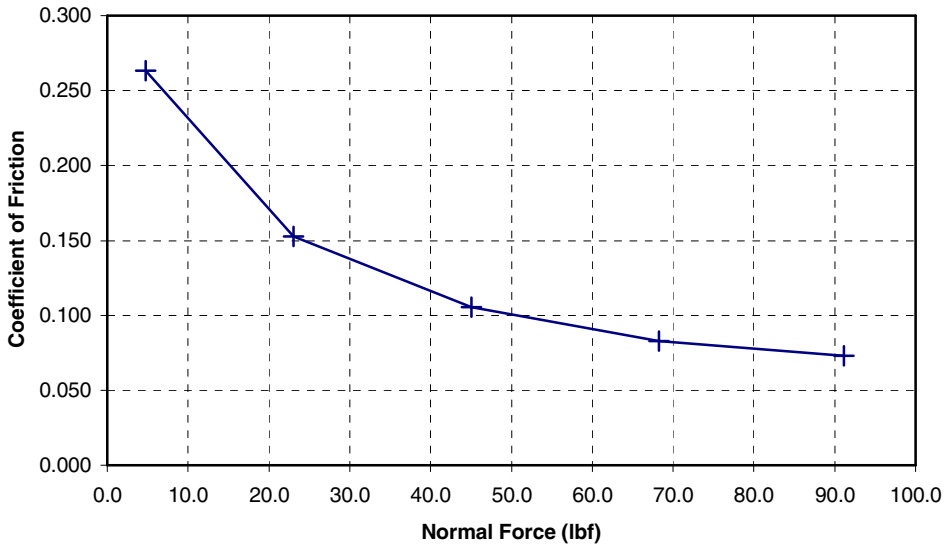

Figure 18 Coefficient of Dynamic Friction vs. Normal Force

6.2 Derive Relationship between Normal Force and Cylinder Pressure

With a prediction of the frictional coefficient in place, the other parameter that is lacking in the model is normal force, F_n. During the analysis of the FEA models, it was observed that the normal force was linearly proportional to the axial force, F_{ax}. Recall that the axial force is the force in the direction of the axis of the piston rod and that it acts on the face of the rod seal that contacts the gland seal groove area A_r. As described in Section 6.1 of this chapter, as well as Chapter 1, the axial force is equal to the product of the cylinder pressure multiplied by the area A_r. This being the case, the

normal force is linearly proportional to the cylinder pressure. This evaluation uses the linear correlation between the normal force and the axial force. The chart shown in Figure 19 depicts the relationship between F_n and F_{ax}. The slope of the least-squares line built upon these data points is the gain term relating F_n and F_{ax}. This gain term is referred to herein as the "area deformation gain".

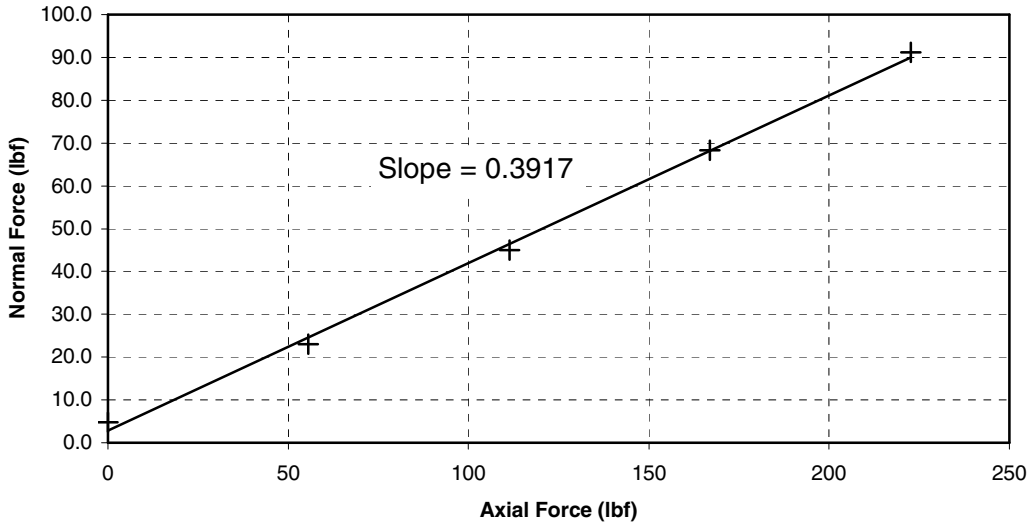

Figure 19 Normal Force vs. Axial Force

With the normal force and the coefficient of dynamic friction characterized, the friction model can be built.

CHAPTER 7

STATIC AND DYNAMIC SIMULATION MODEL

As stated in Chapter 3, the primary objective of this evaluation is to develop a dynamic model whereby seal friction may be predicted in a hydraulic actuator rod seal. The friction model has been developed using test and analytical methods. The key parameters in determining seal friction are listed in Table 5.

Table 5 Key Parameters

Input Parameters	**Nomenclature / Description**
P	Pressure (Variable)
Gland I.D.	Rod Gland Seal Groove Inner Diameter (Constant)
Rod O.D.	Piston Rod Outer Diameter (Constant)
Seal I.D.	Seal Inner Diameter (Constant)
E	Seal Modulus of Elasticity (Constant)
T	Seal Thickness (Constant)
V	Relative Velocity between Piston Rod and Seal (Variable)
ΣF	Sum of the External Forces (Variable)

Output Parameters	**Nomenclature / Description**
f_c	Coulomb Friction (Variable)
F_f	Friction Force - All Friction States Included (Variable) (1)

The key input parameters are used to determine the output parameters as follows:

$$A_r = \frac{\pi}{4}\left((Gland\ I.D.)^2 - (Rod\ I.D.)^2\right)$$

$$F_{ax} = PA_r$$

$$F_{rad} = (Described\ in\ Chapter\ 4)$$

$$F_n = F_{ax}(Area\ Deformation\ Gain) + F_{rad}$$

$$f_c = F_n \mu$$

$$\mu = (Defined\ at\ multiple\ F_n\ values)$$

$$F_f = \begin{cases} f_c Sign(V), & |V| > 0 \\ f_c Sign(\Sigma F), & |V| = 0\ and\ |\Sigma F| \geq f_c \\ \Sigma F, & V = 0\ and\ |\Sigma F| < f_c \end{cases}$$

The preceding values apply over a range of pressure, velocity, and summed force conditions. The equations were programmed into a computer code for stand-alone friction calculation, as well as versatile insertion into a dynamic actuator simulation. Visual representations of the program are given in Figures 20 and 21. Figure 20 shows the calculation of the Coulomb friction F_c. Figure 21 shows the logic used for determining the dynamic friction force F_f with Coulomb friction, relative piston / seal velocity, and summed forces as inputs.

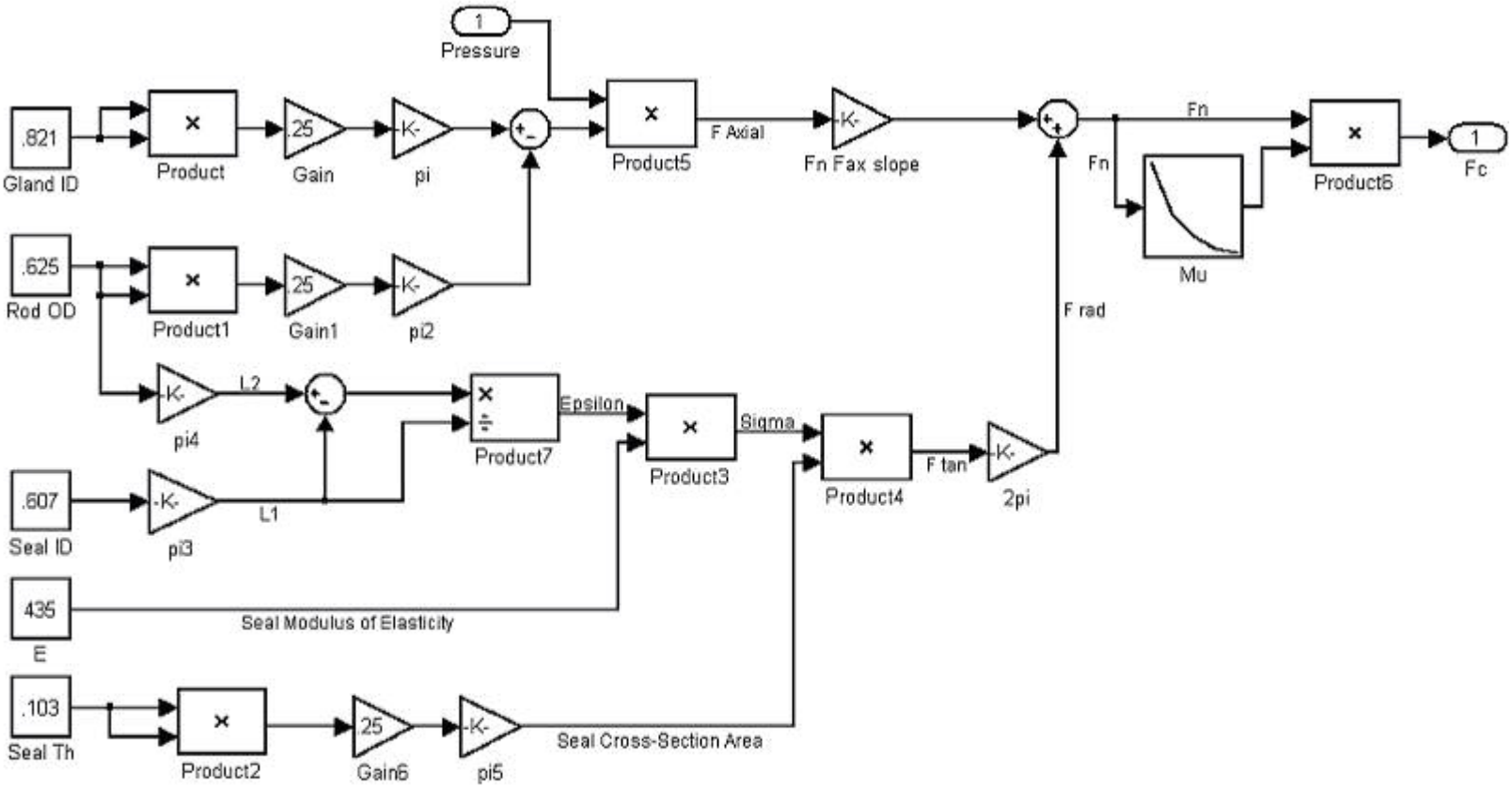

Figure 20 Coulomb Friction Model

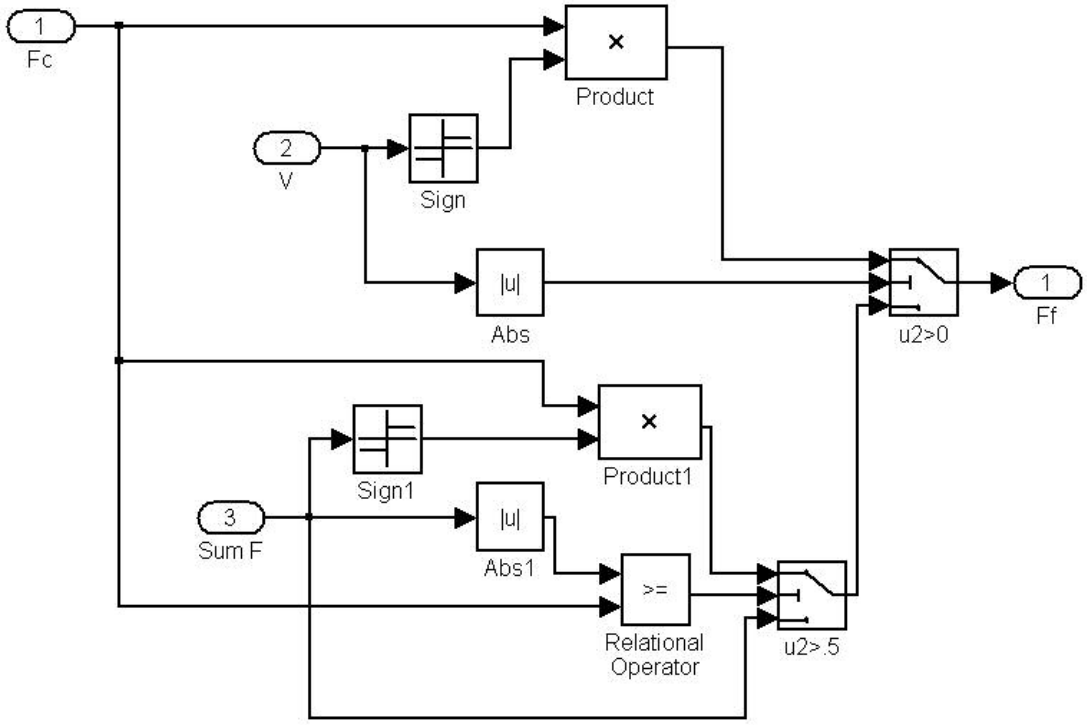

Figure 21 Friction State Model

The logic used in Figure 21 is illustrated using two graphs. The first is created by running the model with a constant pressure, and therefore, a constant Coulomb friction force value. This will be referred to as "friction state 1". Velocity is varied from negative to positive. The results are then plotted with velocity on the X-axis and friction force on the Y-axis. Figure 22 shows these results with a constant cylinder pressure of 500 psi and a velocity that varied from –5 to 5 inches per second.

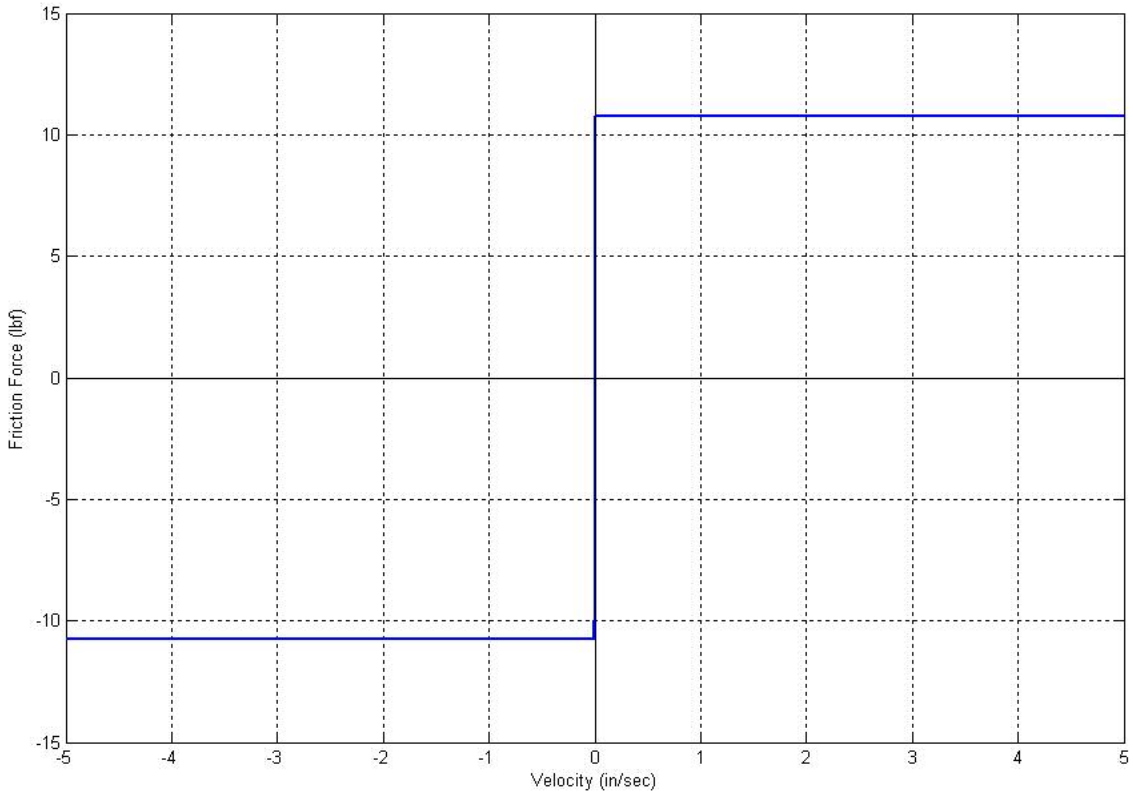

Figure 22 Friction State 1 (Nonzero Velocity)

The second graph (Figure 23) used to illustrate the friction logic of Figure 21 shows two states, referred to as "state 2" and "state 3". State 2 is when the absolute value of the summed external forces is greater than the Coulomb friction force. In this case, the resultant friction force F_f becomes the coulomb friction force multiplied by the sign of the summed external forces. State 3 is also shown on Figure 23. When the absolute value of the summed external forces is less than the Coulomb friction force, the output friction force F_f is equal to the summed external forces.

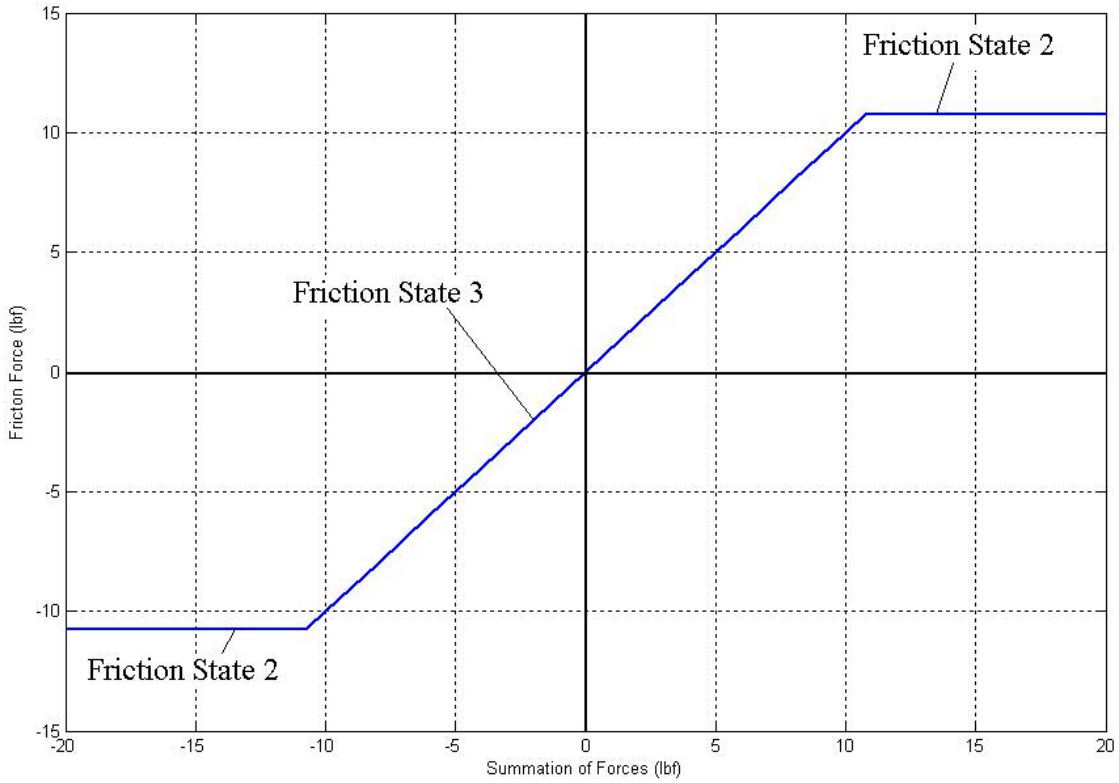

Figure 23 Friction States 2 and 3 (Zero Velocity)

Now that the friction states are established and the equations behind the normal force calculation are developed, the Coulomb friction can be used as a variable input within the model. This value is dependent upon cylinder pressure as the primary variable input. Figure 24 is a plot of the dynamic friction model as it varies with pressure. The friction test data is overlaid for reference.

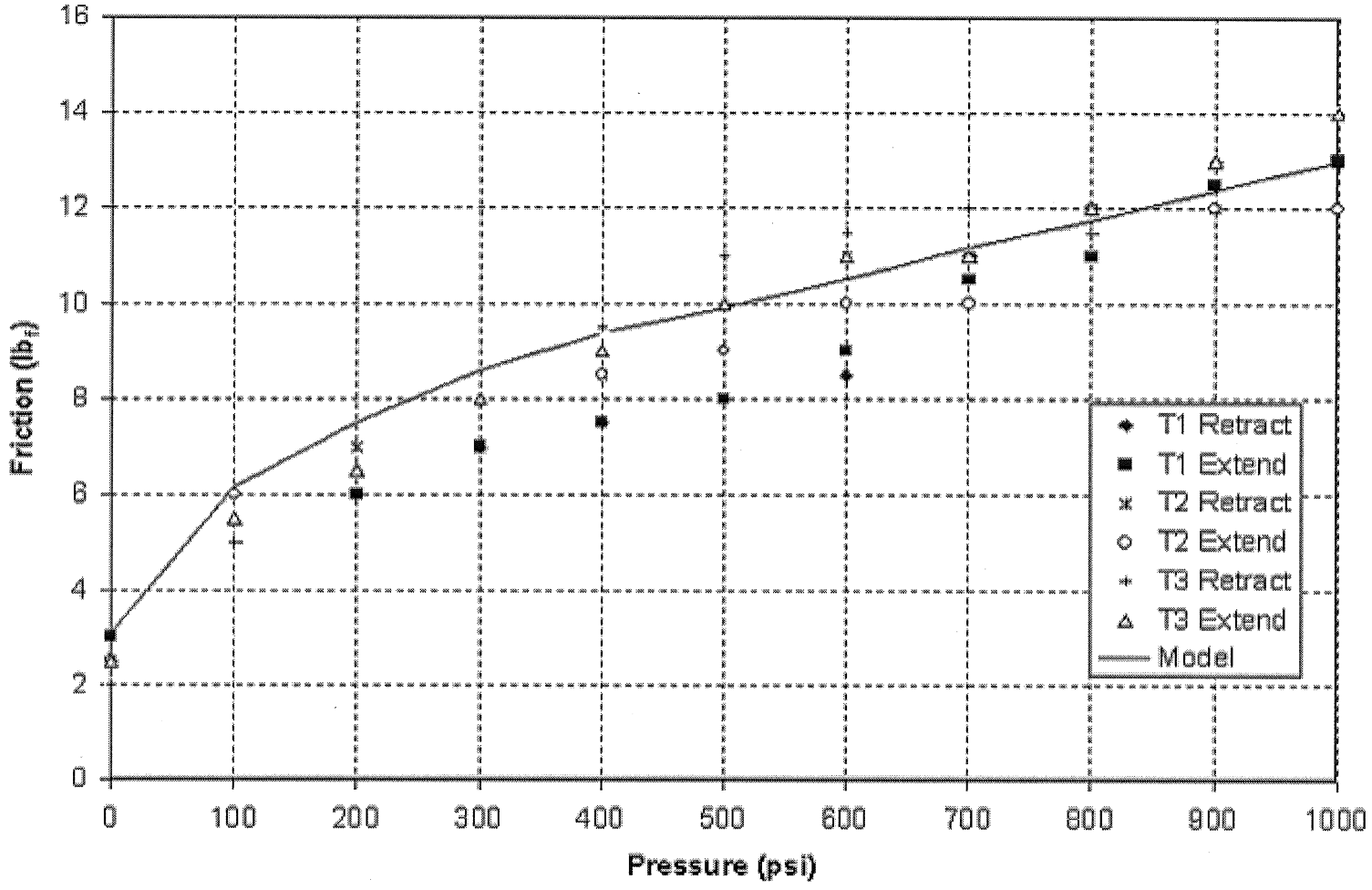

Figure 24 Friction Model Compared with Test Data

Note that between the pressures of 100 and 400 psi, the model overpredicts the friction values as shown by the test data. This is likely due to the linear interpolation of the normal forces found in the FEA models and represents a 5.7% deviation from the average test friction value at the worst case of 200 psi cylinder pressure. The FEA models were performed for five discrete cylinder pressure values (0, 250, 500, 750, and 1000 psi), so the resultant normal forces were interpolated for the case 200 psi cylinder pressure.

The friction model was incorporated into a position control servo simulation for validation. A servo model was chosen such that the friction effects were significant when compared with the output force of the system. A high frequency, low amplitude signal was used as the input. Following the simulation an identical system was modeled with the friction left out. A qualitative output position plot is given in Figure 25. The effects of the friction model are seen in the case with the friction included. As the pressure is reduced on the actuator and the piston comes closer to its direction-reversal point, the friction force becomes greater than the summed forces on the piston. This causes the piston motion to stop, creating the flat peaks on the waveform in Figure 25. As the pressure increases and the summed forces on the piston overcome the Coulomb friction force on the seals, the motion resumes.

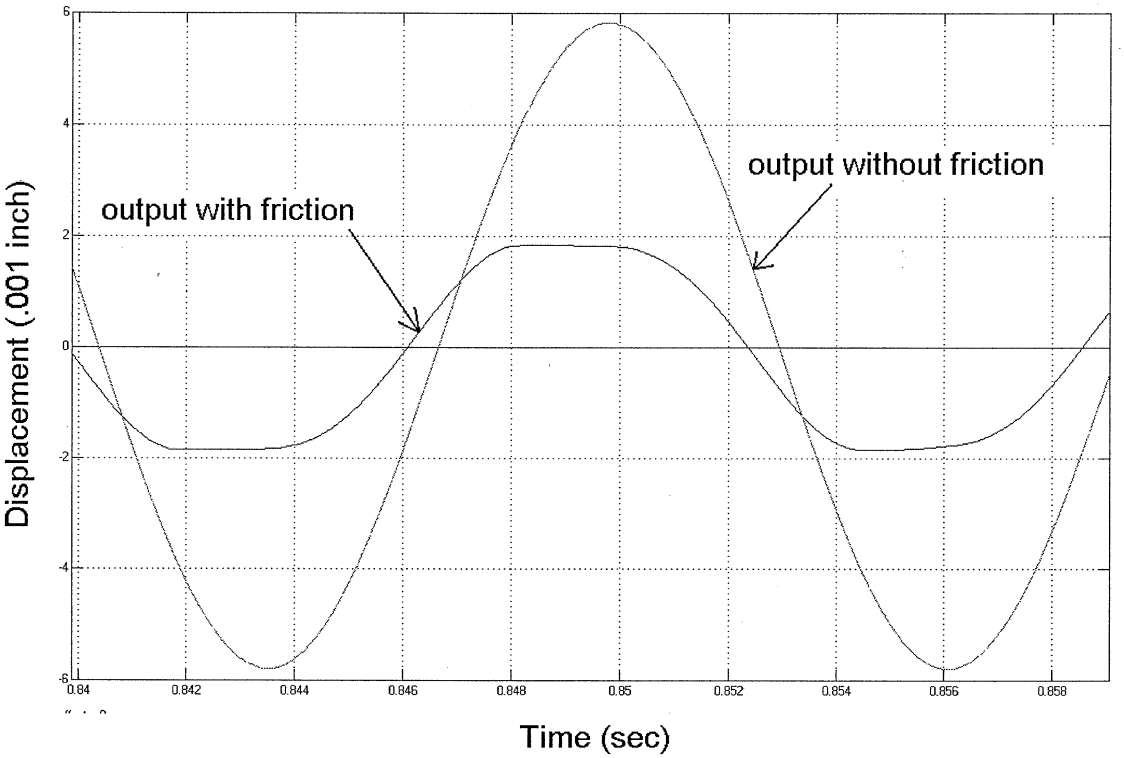

Figure 25 Comparison of Hydraulic Position Servo with and without Friction

CHAPTER 8

CONCLUSIONS AND RECOMMENDATIONS FOR FURTHER RESEARCH

The simulation of hydraulic dynamic seal friction is dependent upon a wide array of factors, but can be modeled with a reasonable level of accuracy. The system must be well understood before an attempt to incorporate the model should be made. While the use of test data is still relevant in the development of this friction model, the information gained can be applied to a variety of O-ring sizes. If desired, the user may take the relationship between friction coefficients and contact stress at each finite element "cell" and apply it to other FEA models. This model can be applied to sealing systems with different seal sizes, seal materials, gland seal groove dimensions, piston rod dimensions, etc.

The subject friction model of this thesis can be taken in its modular form and applied to a dynamic actuator simulation with little effort. Using the inputs of velocity, summed forces, and cylinder pressure within the actuator model, the user can incorporate the effects of friction on a dynamic closed-loop hydraulic control system.

This friction model evaluation covers a range of considerations that must be made when modeling O-ring friction. However, there are many other phenomena that occur within a sealing system. Other topics for research may include duration of contact between the seal and the sealing surface, piston rod surface finish parameters, fluid composition and journal effects, Coulomb friction at varied velocities, and more detailed procedures for scaling the model at different seal sizes. Other parameters that

will have an effect on the seal friction and should be investigated include temperature, seal age, type of seal (non-circular cross-section), and composite seals (PTFE seals with elastomeric energizers).

Another suggested topic of research and analysis sequential to this thesis is the formulation of FEA models to determine friction coefficients as a function of localized contact stress. This will require multiple FEA models, but will yield a relationship that may be used to further automate the construction of the subject friction model.

APPENDIX A

FRICTION MEASUREMENT TEST PLAN

Seal Friction Measurement Test Plan

Equipment

- Balanced-area hydraulic piston / cylinder assembly
- Cylinder grounding fixture
- Hydraulic hoses and fittings as required
- 0-1000 psi pressure gage
- Trunnion strap
- Load measurement device (load cell, spring scale, or weighted pulley)
- Hydraulic pressure supply

Test Procedure

1. Measure and record piston rod and seal groove dimensional information.
2. Set up the piston / cylinder assembly and related equipment as shown in Figure A-1.
3. Apply 100 psig to pressure port.
4. Bleed air from the system.
5. Bring pressure to 0 psig.
6. Allow assembly to sit for thirty seconds.
7. Using the load measurement device, push on the cylinder until it begins to move. Measure and record the pressure and the force required to cause the cylinder to move, as well as the running friction.
8. Repeat step 7, pulling the cylinder instead of pushing.
9. Repeat steps 6 through 8 ten times, raising the pressure in 100 psi increments each time.
10. Repeat steps 6 through 9 twice for validation of previously recorded values.

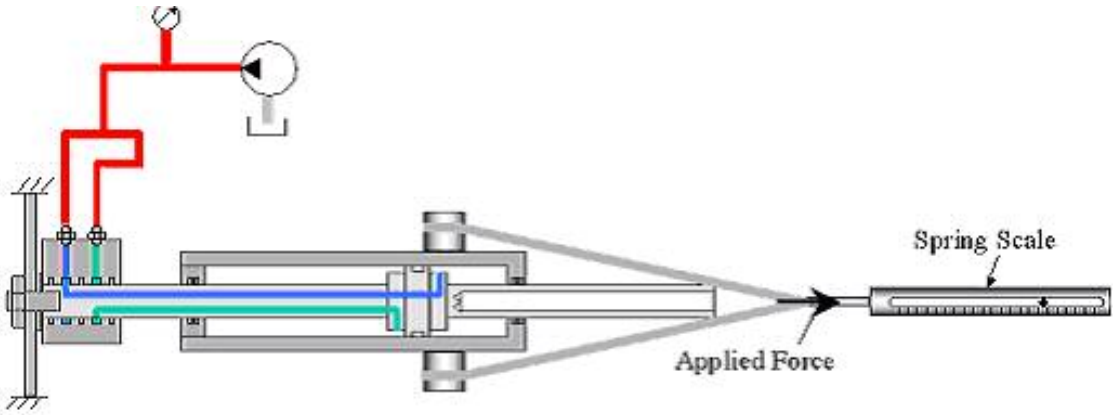

Figure A-1 Test Setup

Gland Seal Groove I.D.: _____inch
Piston Rod O.D.: _____inch
Seal I.D.: _____inch
Seal Thickness: _____inch

Pressure (psig)	Test 1 Static Friction (lbf)		Test 1 Dynamic Friction (lbf)		Test 2 Static Friction (lbf		Test 2 Dynamic Friction (lbf)		Test 3 Static Friction (lbf)		Test 3 Dynamic Friction (lbf)	
	Ret	Ext	Ret	Ext	Ret	Ext	Ret	Ext	Ret	Ext	Ret	Ext
0												
100												
200												
300												
400												
500												
600												
700												
800												
900												
1000												

Figure A-2 Test Specimen

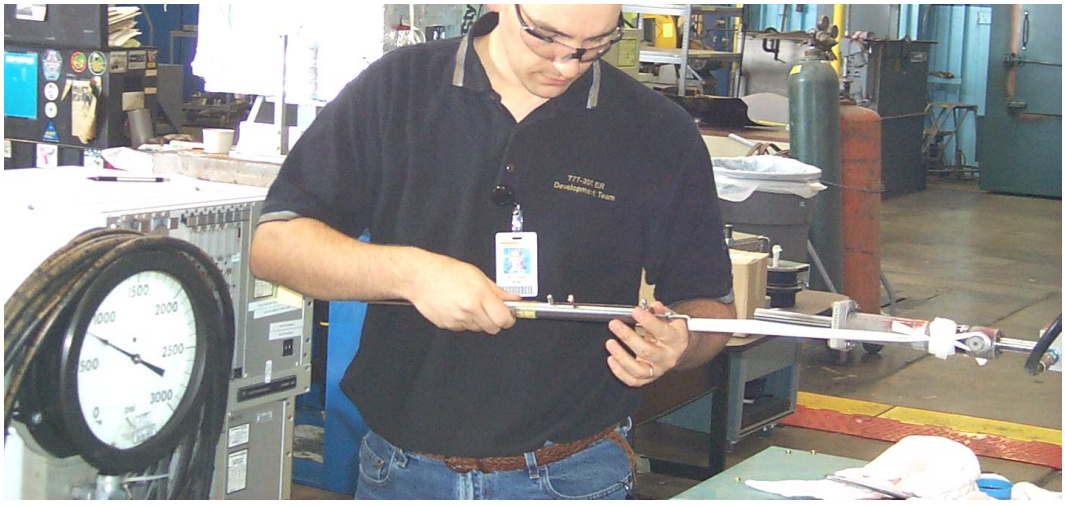

Figure A-3 Friction Test

Table A-1 Friction Test Data – Test 1

	Test 1			
	Static Friction (lb_f)		Dynamic Friction (lb_f)	
Pressure (psig)	***Retract***	***Extend***	***Retract***	***Extend***
0	3.0	3.5	2.5	3.0
100	6.0	6.0	5.0	5.0
200	7.0	7.0	6.0	6.0
300	8.0	8.0	7.0	7.0
400	8.0	8.0	7.5	7.5
500	9.0	8.5	8.0	8.0
600	10.0	10.5	8.5	9.0
700	12.0	11.0	11.0	10.5
800	13.0	12.0	11.5	11.0
900	14.0	12.5	13.0	12.5
1000	14.0	14.0	13.0	13.0

Table A-2 Friction Test Data – Test 2

	Test 2			
	Static Friction (lb_f)		Dynamic Friction (lb_f)	
Pressure (psig)	***Retract***	***Extend***	***Retract***	***Extend***
0	3.0	2.5	2.5	2.5
100	7.0	6.5	5.0	6.0
200	8.5	7.0	7.0	6.5
300	10.0	9.0	8.0	8.0
400	10.0	9.0	8.5	8.5
500	11.5	9.5	11.0	9.0
600	12.5	10.0	11.0	10.0
700	13.0	11.0	11.0	10.0
800	14.0	13.0	12.0	12.0
900	16.0	13.0	12.0	12.0
1000	17.0	13.0	14.0	12.0

Table A-3 Friction Test Data – Test 3

	Test 3			
	Static Friction (lb_f)		Dynamic Friction (lb_f)	
Pressure (psig)	***Retract***	***Extend***	***Retract***	***Extend***
0	3.5	2.5	2.0	2.5
100	6.0	6.5	5.0	5.5
200	8.0	7.0	6.5	6.5
300	9.5	8.5	8.0	8.0
400	11.0	9.5	9.5	9.0
500	13.0	10.5	11.0	10.0
600	12.5	11.5	11.5	11.0
700	14.0	12.0	12.0	11.0
800	12.0	12.5	11.5	12.0
900	16.0	15.0	13.0	13.0
1000	17.0	15.0	14.0	14.0

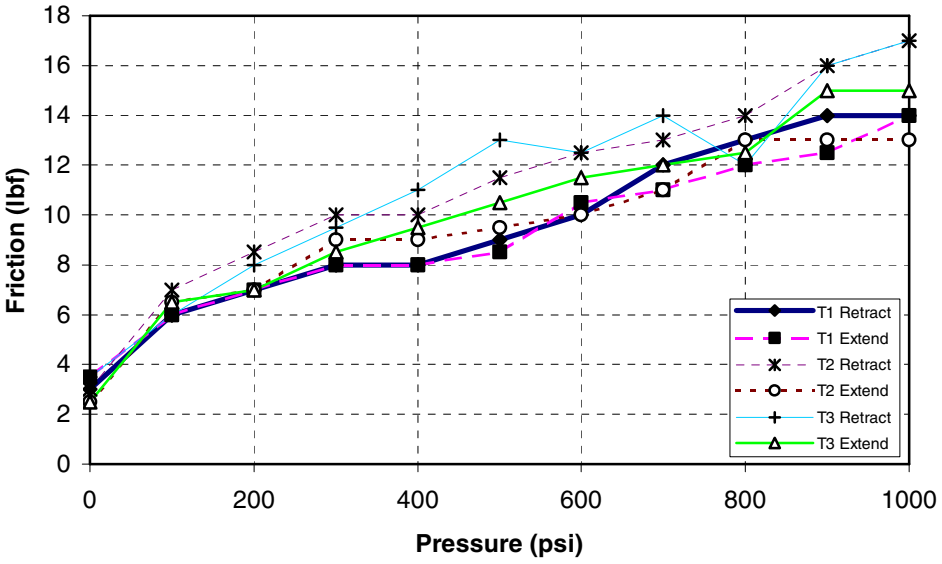

Figure A-4 Static Friction vs. Pressure

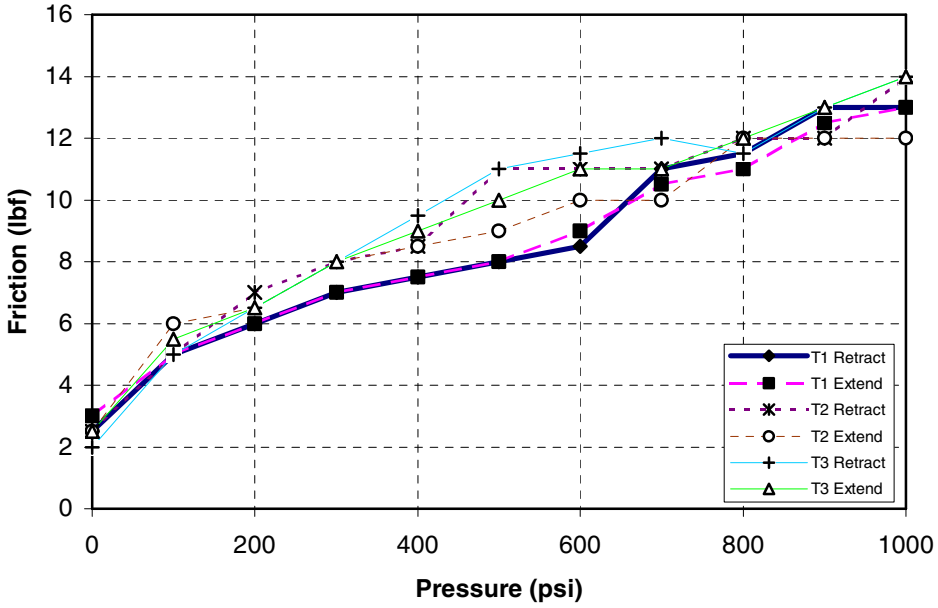

Figure A-5 Dynamic Friction vs. Pressure

APPENDIX B

FINITE ELEMENT ANALYSIS RESULTS

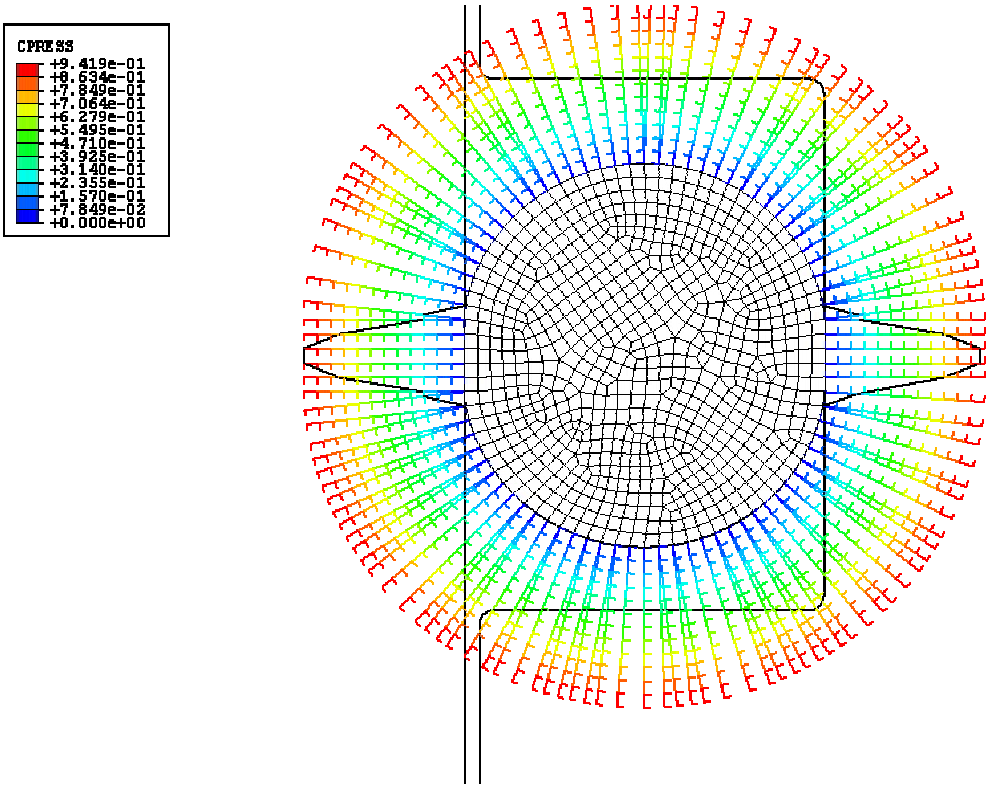

Figure B-1 Contact Stress Due to O-Ring Seal Installation Squeeze

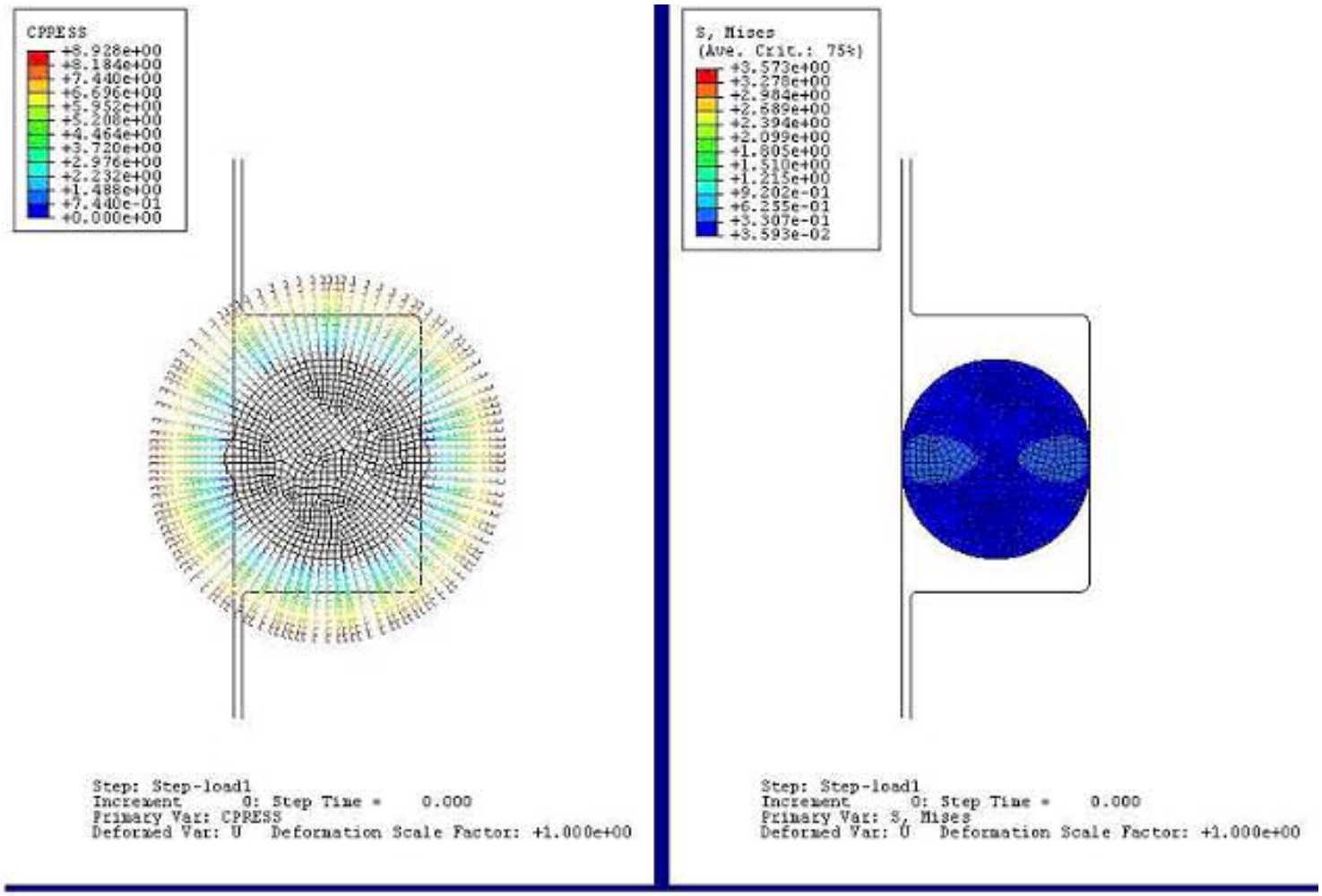

Figure B-2 Contact and Von Mises Stress, Cylinder Pressure = 0 psi

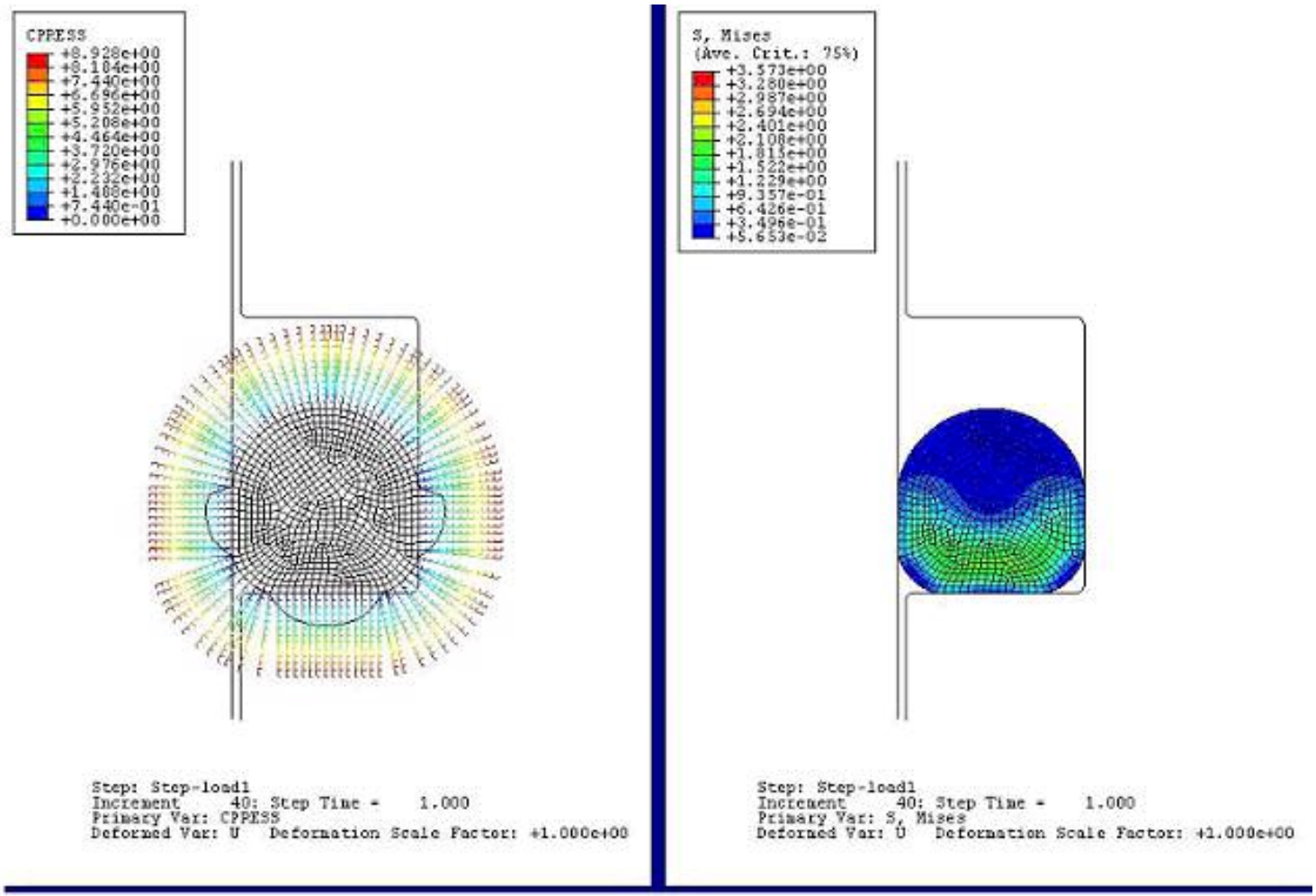

Figure **B-3** Contact and Von Mises Stress, Cylinder Pressure = 250 psi

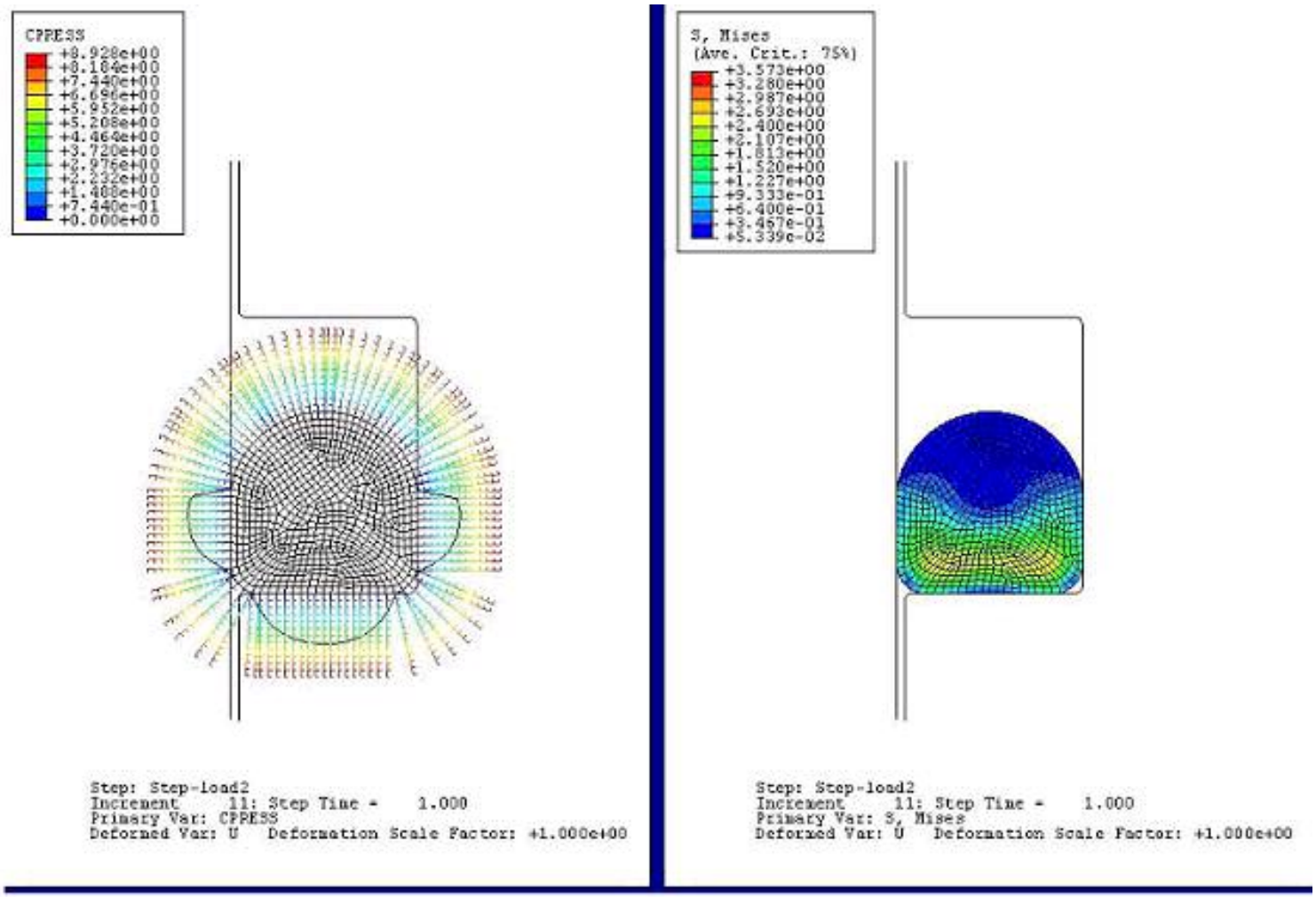

Figure B-4 Contact and Von Mises Stress, Cylinder Pressure = 500 psi

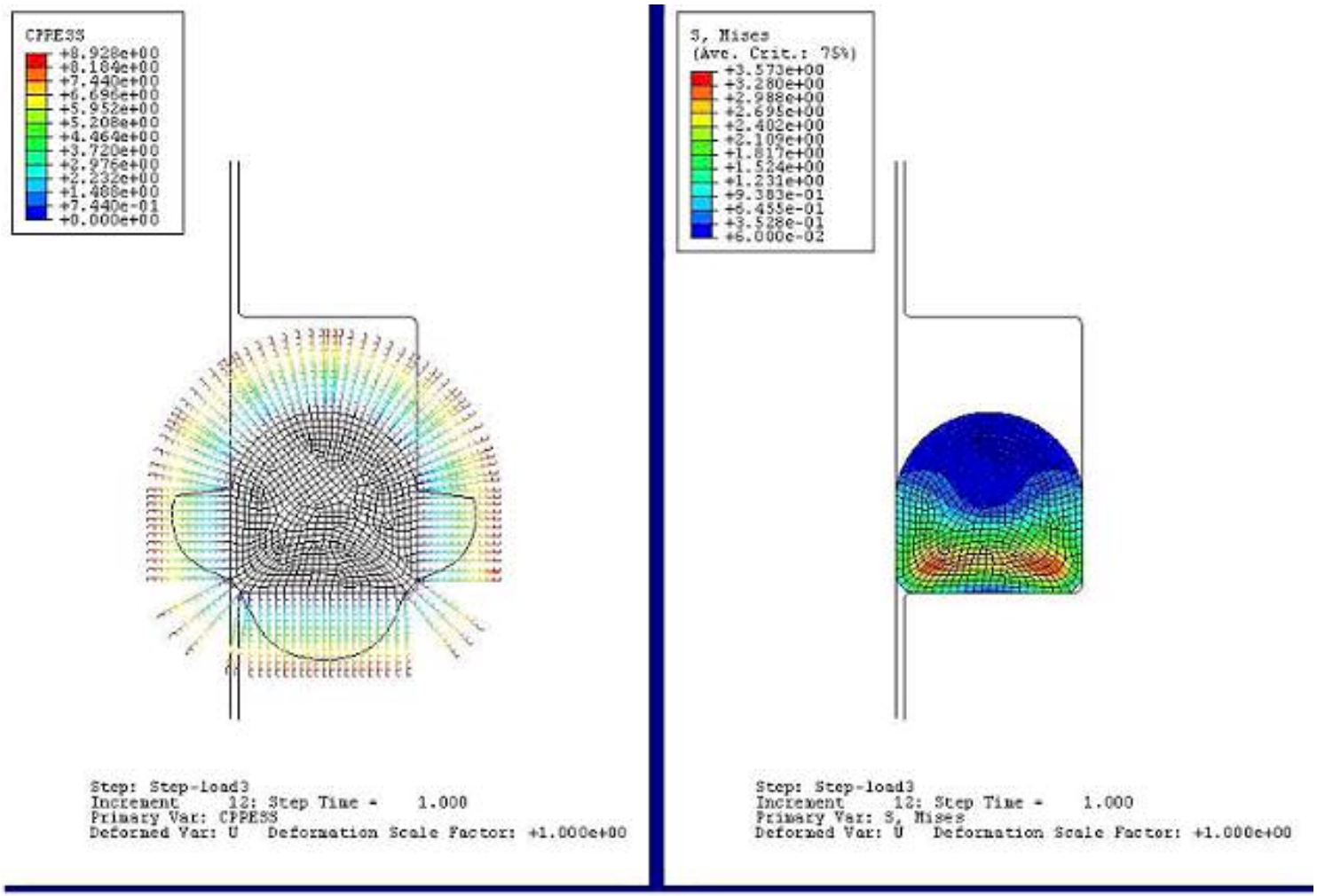

Figure **B-5** Contact and Von Mises Stress, Cylinder Pressure = 750 psi

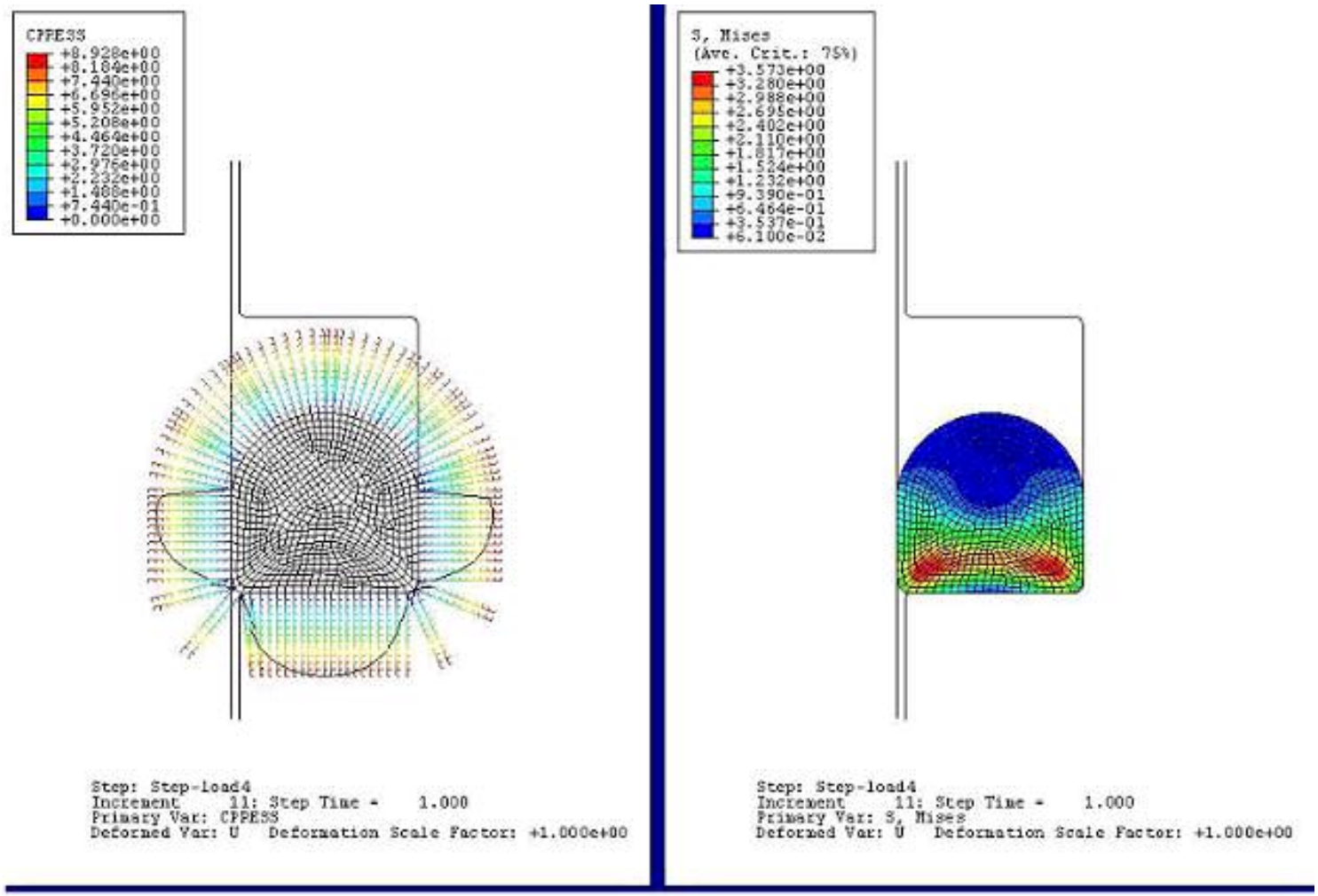

Figure B-6 Contact and Von Mises Stress, Cylinder Pressure = 1000 psi

Cylinder Pressure	0 psig
Piston Contact Length	0.026 in
Cell Contact Area	0.00729 in^2
A_r	0.223 in^2
F_{ax}	0.0 lb_f

Node Position	Contact Stress (psi)	Cell Force (lb_f)
0.0019	17.1	0.125
0.0056	71.2	0.519
0.0093	122.4	0.893
0.0130	136.6	0.997
0.0167	122.4	0.893
0.0204	71.2	0.519
0.0241	17.1	0.125

F_n (lb_f)	4.1

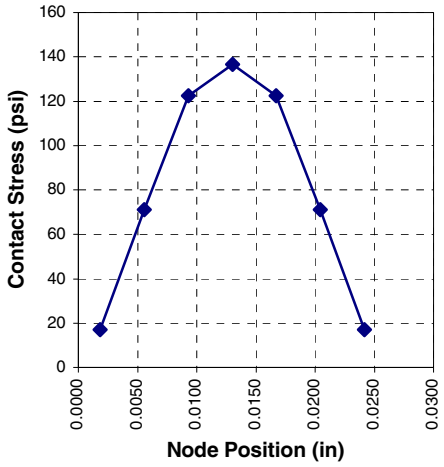

Figure B-7 FEA Contact Stress, Axial Force, and Normal Force, Cylinder Pressure = 0 psig

Cylinder Pressure	250 psig
Piston Contact Length	0.037 in
Cell Contact Area	0.00810 in^2
A_r	0.223 in^2
F_{ax}	55.8 lb_f

Node Position	Contact Stress (psi)	Cell Force (lb_f)
0.0021	183.5	1.486
0.0062	388.6	3.147
0.0103	415.6	3.366
0.0144	421.0	3.410
0.0185	404.8	3.279
0.0226	364.3	2.951
0.0267	304.9	2.470
0.0308	210.5	1.705
0.0349	75.6	0.612

F_n (lb_f)	22.4

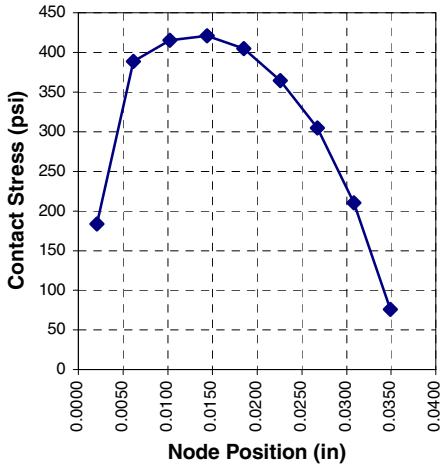

Figure B-8 FEA Contact Stress, Axial Force, and Normal Force, Cylinder Pressure = 250 psig

Cylinder Pressure	500 psig
Piston Contact Length	0.046 in
Cell Contact Area	0.00830 in^2
A_r	0.223 in^2
F_{ax}	111.5 lb_f

Node Position	Contact Stress (psi)	Cell Force (lb_f)
0.0021	296.8	2.464
0.0063	620.6	5.151
0.0105	653.0	5.420
0.0146	658.4	5.465
0.0188	653.0	5.420
0.0230	636.8	5.286
0.0272	599.1	4.972
0.0314	528.9	4.390
0.0355	412.9	3.427
0.0397	234.8	1.949
0.0439	64.8	0.538

F_n (lb_f)	44.5

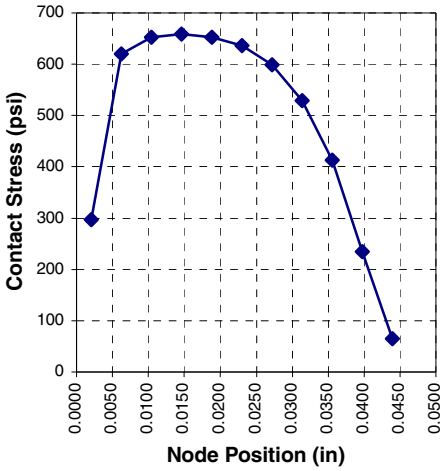

Figure B-9 FEA Contact Stress, Axial Force, and Normal Force, Cylinder Pressure = 500 psig

Cylinder Pressure	750 psig
Piston Contact Length	0.051 in
Cell Contact Area	0.00830 in^2
A_r	0.223 in^2
F_{ax}	167.3 lb_f

Node Position	Contact Stress (psi)	Cell Force (lb_f)
0.0021	431.8	3.584
0.0064	874.3	7.257
0.0106	895.9	7.436
0.0149	904.0	7.503
0.0191	898.6	7.458
0.0234	885.1	7.346
0.0276	855.4	7.100
0.0319	801.4	6.652
0.0361	698.9	5.801
0.0404	531.6	4.412
0.0446	269.8	2.240
0.0489	54.0	0.448

F_n (lb_f)	67.2

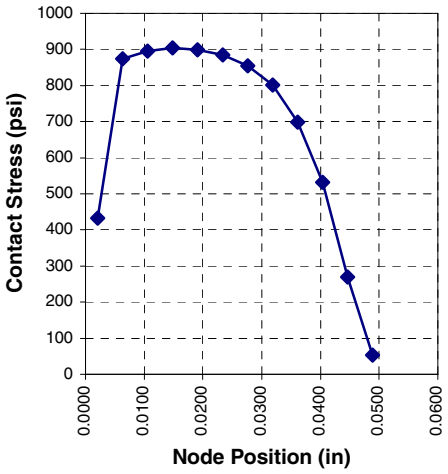

Figure B-10 FEA Contact Stress, Axial Force, and Normal Force, Cylinder Pressure = 750 psig

Cylinder Pressure	1000 psig
Piston Contact Length	0.05 in
Cell Contact Area	0.00820 in^2
A_r	0.223 in^2
F_{ax}	223.0 lb_f

Node Position	Contact Stress (psi)	Cell Force (lb_f)
0.0021	107.9	0.885
0.0063	1102.6	9.041
0.0104	1160.6	9.517
0.0146	1187.3	9.736
0.0188	1187.3	9.736
0.0229	1167.9	9.577
0.0271	1138.9	9.339
0.0313	1088.1	8.922
0.0354	1025.4	8.408
0.0396	891.4	7.309
0.0438	701.6	5.753
0.0479	350.4	2.873

F_n (lb_f)	91.1

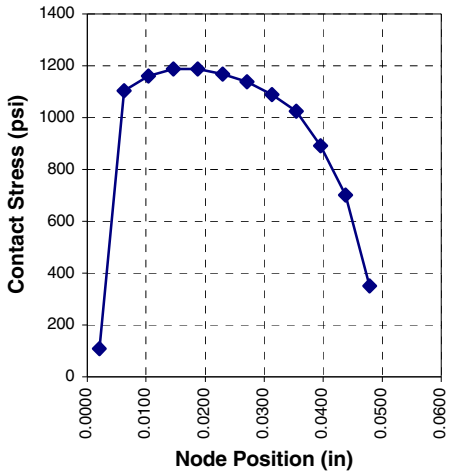

Figure B-11 FEA Contact Stress, Axial Force, and Normal Force, Cylinder Pressure = 1000 psig

REFERENCES

(1) Woods, R. L. (2005). Coulomb Friction Between Two Moving Bodies Including Static and Dynamic Motion, 1-3.

(2) Thoman, R. A. Jr. (1992). An Empirical Approach to Seal Friction. SAE Technical Paper Series, 922015, 1-5.

(3) Parker Hannifin Corporation (2001). Parker O-Ring Handbook (2001 Edition) Cleveland, OH: Parker Hannifin Corporation

(4) Gere, J. M. and Timoshenko, S. P. (1997). Mechanics of Materials (4^{th} ed.) Boston, MA: PWS Publishing Company (557).

BIOGRAPHICAL INFORMATION

The author earned a B.S. in Mechanical Engineering from Utah State University. One year of his graduate program was completed at University of Utah, with special emphasis on computational fluid dynamics and internal flow analysis. The second year of his graduate program was completed at University of Texas at Arlington, with an emphasis on fluid power control systems. This thesis is the final requirement for a M.S. in Mechanical engineering. He is currently employed with Bell Helicopter in the fixed controls and hydraulics group, designing helicopter flight control actuation and hydraulic systems.